TECHNICAL MEMORANDUMS

NATIONAL ADVISORY COMMITTEE FOR AERONAUTICS

No. 603

WRINKLING OF REINFORCED PLATES SUBJECTED TO SHEAR STRESSES

By Edgar Seydel

Jahrbuch 1930 der Deutschen Versuchsanstalt
für Luftfahrt e.V., Berlin-Adlershof
Verlag von R. Oldenbourg, München-Berlin, 1930

Washington
January, 1931

NATIONAL ADVISORY COMMITTEE FOR AERONAUTICS

TECHNICAL MEMORANDUM No. 602

WRINKLING OF REINFORCED PLATES SUBJECTED TO SHEAR STRESSES*

By Edgar Seydel

R e s u m e

It is common practice to stiffen flat plates by ribs or special shaping (corrugations). Now in many load cases the principal stress in a plate is the shear which, upon reaching a certain limit, the so-called critical load, forces the plate to wrinkle.

When these reinforcements are appropriately applied the stiffened plate can be treated as a homogeneous plate (orthogonal-anisotropic) with uniformly and closely spaced reinforcements (different in both directions), and the formula for buckling in shear is deduced from a differential equation of the fourth order. By introducing the characteristic value of the orthogonal-anisotropic plate and applying further appropriate parameters the solution can be carried out for a plate strip of great length by arbitrary plate stiffeners. The edges may be freely supported or rigidly constrained.

---

*"Beitrag zur Frage des Ausbeulens von versteiften Platten bei Schubbeanspruchung." From Jahrbuch 1930 der Deutschen Versuchsanstalt für Luftfahrt e.V., Berlin-Adlershof - Verlag von R. Oldenbourg, München-Berlin 1930, pp. 235-254.

Introduction

The buckling strength in shear (and the vibration) of long, thin, isotropic plates supported at the long edges has been treated quite exhaustively by R. V. Southwell and S. W. Skan (Reference 1). St. Bergmann and H. Reissner (Reference 2) extended Southwell's theory to include the case of anisotropic (orthogonal-anisotropic) plates with vanishing and comparably low bending stiffness longitudinally. Their data are included in this report. C. Schmieden (Reference 3) treats the case of equal longitudinal stiffness in bending and distortion, but his methods were incomprehensible to me and his data are confirmed only for the case of infinitely low distortion stiffness.

M. T. Huber (Reference 4) established the theory and the general differential equation of bending in orthogonal-anisotropic plates.

In the present report the problem of buckling strength and lobed form of failure of anisotropic plate strips is carried to a certain conclusion and the data for arbitrary stiffness in bending in two directions at right angles to each other, and for arbitrary distortion stiffness is exhibited diagrammatically. For the suggestions on this report and helpful advice I am indebted to Professor H. Reissner.

P r o b l e m

1. The system (the reinforced plate).- The thin plate (metal or plywood) is a structural element which finds extensive use in airplane construction. Among others it is intended to form a substitute for bracing and for that reason it is in many load cases chiefly subjected to shear. The low stiffness of the thin plate which induces bulging (lobing, wrinkling) even under relatively low shear stresses, and the inability to absorb compression and bending stresses, necessitates reinforcements. This stiffening can be accomplished with riveted or glued strips (ribs), or by special shaping (corrugated plate), usually in one or two directions.

Wrinkling is an elastic form change in which deflections and distortions occur in the originally flat plate center, and depends therefore on the stiffness in bending and distortion of the plate.

This stiffness (with respect to unit length) of the homogeneous isotropic plate, being the same at every point and in every direction, is higher at the reinforcements than at the non-reinforced points. In addition, the bending stiffness (depending on shape of reinforcement) is usually different in different directions of the stiffened plate.

If the reinforcements are equally spaced and under certain circumstances of equal thickness, the stiffness (with respect to unit length) is periodically variable along the two axes.

A flat plate may be visualized as taking the place of a corrugated sheet (located in the ideal median plane of the corrugated sheet), whose stiffness corresponds at every point with that of the corrugated sheet. In this case the stiffness again is subject to periodic changes - here, continuous - while in the plate with reinforcing strips the cross sectional inertia moments and through them, the stiffness changes irregularly (at least, when making the usual simplifying assumptions regarding the stress of a beam in bending). Thus, the stiffened plate represents, even if it consists of isotropic material, a non-homogeneous system, because the elastic properties of the plate are not the same at every point. But we speak of a mean bending stiffness in one and in the other direction (parallel and at right angles to the direction of the reinforcing strip). Hence, we must distinguish between the mean bending stiffness D_1, and the mean bending stiffness D_2, with respect to two axes given by the direction of the reinforcements, and which may be assumed as the x and y axes of a system placed in the (ideal) median plane of the reinforced plate. Hereby D_1 is the bending stiffness corresponding to the stress in bending σ_x in the x-direction, and D_2 conformal to the normal tension σ_y. In this manner we arrive at an idealized homogeneous plate system whose elastic properties are different in two directions, which, in fact, is conformal to a flat nonreinforced plate of orthogonal-anisotropic material (originally, isotropic -

or, better, quasi-isotropic material when rolled, assumes such qualities to a slight extent).

Now, when the periods of the stiffness-change of an actually reinforced plate are sufficiently small, the elastic surface of this nonhomogeneous plate in bending (and distortion) deflection differs only slightly from the elastic surface of the corresponding homogeneous orthogonal-anisotropic plate, and we may speak of a quasi-homogeneous system. Hereby it should be borne in mind that the periods of stiffness-change must not only be small with respect to the plate length, but also be so small that the elastic surface of the ideal system conforms to the actually existing system.

Disregarding the transverse elongation with its trifling and frequently negligible effect, the bending stiffness is the product of the Young's modulus of the material and the (mean) inertai moment of the reinforced plate section per unit length. The determination of the distortion stiffness requires an examination of the elastic form changes of the reinforced plate, where it is assumed that only shear moments (no bending moments) act in every intersection parallel to the x-axis and parallel to y-axis, due to the load being applied to the edges. As a rule, the stiffeners do not materially raise the distortion stiffness of a flat plate when the reinforcing strips are small in comparison to their spacing, although the edge attachment of a corrugated plate seems to affect its distortion stiffness considerably.

The present report is confined to the rectangular plate of (infinitely) great length (in the x-direction) and of $2a$ width (in the y-direction). The stiffeners are parallel to the edges, and the plate thickness δ is small with respect to the width. At the edges $y = \pm a$ the plate is freely supported or rigidly constrained.

2. Loading.- Such a strip is subjected to an evenly distributed constant shear t, per unit length, which acts along the four edges in the median plane of the plate and is in outside equilibrium. The result is a constant shear stress in the whole quasi-homogeneous plate.

While t is low the plate remains flat, but as the shear increases and finally becomes maximum, the plate reaches its so-called shear strength t_{kr}, and upon exceeding this critical limit, the plate wrinkles. Figure 1 shows the basic form (contours and cross sections) which the elastic surface assumes by incipient wrinkling. (This elastic surface is discussed in a subsequent section (III). It depends on the ratio of bending and distortion stiffness and the boundary conditions.) The stress attitude of the plate changes, bending and normal stresses occur, the plate attempts to assume a new attitude of equilibrium, but fails if the ultimate strength is exceeded or local buckling sets in. We begin with the determination of the shear strength t_{kr}.

II. Test Data

3. The shear strength.- Before going into details, we wish to state the result.

The shear strength t_{kr} is computed from one of two formulas:

$$t_{kr} = c_a \frac{\sqrt[4]{D_1 D_2^3}}{a^2} \tag{1a}$$

$$t_{kr} = c_b \frac{\sqrt{D_2 D_3}}{a^2} \tag{1b}$$

or, according to Bergmann and Reissner

$$\frac{t_{kr} a^2}{D_2} = c_a \sqrt[4]{\rho} \tag{1'a}$$

$$\frac{t_{kr} a^2}{D_2} = c_b \sqrt{\mu} \tag{1'b}$$

with

$$\left.\begin{aligned} \frac{D_1}{D_2} &= \rho \\ \frac{D_3}{D_2} &= \mu \end{aligned}\right\} \tag{2}$$

Here a = half width of plate strip,

D_1 = mean stiffness in bending in direction of x (length),

D_2 = mean stiffness in bending in direction of y (width),

D_3 = mean stiffness in distortion (when disregarding the transverse elongation)*

of the reinforced plate, the stiffness is expressed in units of cross sectional width, that is, in kg cm, while c_a and c_b are

*See footnote, next page.

absolute coefficients contingent upon

$$\vartheta = \frac{\sqrt{D_1 D_2}}{D_3} = \frac{\sqrt{\rho}}{\mu} \qquad (3)$$

and which become apparent from Figures 2a and 2b. If $\vartheta > 1$, these figures show that it is preferable to use equation (1a) or (1'a), but if $\vartheta < 1$, that formula (1b) or (1'b) would be more suitable. When the bending stiffness vanishes in the x-direction, that is, if $D_1 = 0$, then $\vartheta = 0$, and formula (1a) yields $t_{kr} = \infty \times 0$, or an indeterminate value, but (1b) and (1'b) give in this case

$$t_{krf} = 11.71 \frac{D_2 D_3}{a^2} = 11.71 \frac{D_2\sqrt{\mu}}{a^2} \quad \text{by free support}$$

and

$$t_{kre} = 18.59 \frac{D_2 D_3}{a^2} = 18.59 \frac{D_2\sqrt{\mu}}{a^2} \quad \text{by rigid restraint}$$

on the edges $y = \pm a$. When the bending stiffness disappears

---

*(Footnote from page 7)
Considering the idealized Poisson's ratio, ν_x and ν_y in the x- and y-direction (compare section VI, formulas (6) and (7)) would yield the more accurate values for the bending stiffness in unit length

$$D_1 = \frac{(EJ)_x}{1-\nu_x \nu_y} \quad \text{in x-direction,}$$

$$D_2 = \frac{(EJ)_y}{1-\nu_x \nu_y} \quad \text{in y-direction,}$$

while D_3 is given by

$$2 D_3 = \nu_x \frac{(EJ)_y}{1-\nu_x \nu_y} + \nu_y \frac{(EJ)_x}{1-\nu_x \nu_y} + 4 (GJ)_{xy}$$

where $2 (GJ)_{xy}$ is the distortion stiffness of the orthogonal-anisotropic plate with respect to the cross-sectional width "one." The definition of ν_x and ν_y is given in section VI.

in the x-direction the shear strength t_{kr}* is therefore not zero (but $D_2 = 0$ yields $t_{kr} = 0$). On the other hand, if the distortion stiffness is $D_3 = 0$, then $\vartheta = \infty$ and, according to (1a) and (1'a)

$$t_{kr\,f} = 8.125 \frac{\sqrt[4]{D_1 D_2^3}}{a^2} = 8.125 \frac{D_2 \sqrt[4]{\rho}}{a^2} \quad \text{by free support,}$$

and

$$t_{kr\,e} = 15.065 \frac{\sqrt[4]{D_1 D_2^3}}{a^2} = 15.065 \frac{D_2 \sqrt[4]{\rho}}{a^2} \quad \text{by rigid restraint,}$$

while (1b) for the time being yields an indeterminate value $\infty \times 0$.

If value ϑ is very large or very small, or, at any rate, much higher or lower than "one," one may figure with the c_a value for $\vartheta = \infty$ and c_b for $\vartheta = 0$, where the t_{kr} figures will be somewhat too low; the error committed here can be seen on Figure 3a where the quotient $c_a/c_{a(\vartheta=\infty)}$ is plotted against ϑ. The shear strength (for $\vartheta > 1$) is computed as

$$t_{kr} = \frac{c_a}{c_{a(\vartheta=\infty)}} 8.125 \frac{\sqrt[4]{D_1 D_2^3}}{a^2} \quad \text{by free support}$$

and

$$= \frac{c_a}{c_{a(\vartheta=\infty)}} 15.065 \frac{\sqrt[4]{D_1 D_2^3}}{a^2} \quad \text{by rigid restraint}$$

where $c_a/c_{a(\vartheta=\infty)}$ slightly exceeds "one," and on Figure 3b with

*Bergmann and Reissner first resolved the problem by assuming $D_1 = 0$. Their value

$$\left(\frac{T}{D_2}\right)_{min} = \frac{8.283 \sqrt{2} \times \sqrt{\mu}}{a^2}$$

is in exact agreement with the above formula. In their second report they showed the initial tangent of the function $c_b = c_b^{(\vartheta^2)}$.

$c_b/c_{b(\vartheta=0)}$ plotted against $1/\vartheta$. Thus the shear strength for $\vartheta < 1$ becomes:

$$t_{kr} = \frac{c_b}{c_{b(\vartheta=0)}} 11.71 \frac{\sqrt{D_2 D_3}}{a^2} \quad \text{(by free support)}$$

and

$$= \frac{c_b}{c_{b(\vartheta=0)}} 18.59 \frac{\sqrt{D_2 D_3}}{a^2} \quad \text{(by rigid restraint)}$$

quotient $c_b/c_{b(\vartheta=0)}$ being slightly higher than "one," when ϑ is materially lower than "one." When $\vartheta = 1$, so that $\rho = \mu$*

*The case $\vartheta = 1$ was examined by Southwell, and our data, although established for the isotropic plate, apply for certain cases of the anisotropic plate as well. Schmieden first treats the case $\rho = \mu(=A)$ and when resolving the problem, confines himself to very small $\rho(=A)$ values. He assumes the κ value, which he denotes by λ, and which is inversely proportional to the wave length of the elastic surface, to be inversely proportional to $\sqrt[4]{\rho}$ $(= \sqrt[4]{A})$ in the case of critical shear load, so that $\kappa_{kr} \sqrt[4]{\rho}$ $(= \lambda \sqrt[4]{A})$ is constant, (i.e., unaffected by ρ). From the special case $\rho = \mu < 1$ he proceeds to the more general case $\mu = 0$, $\rho \neq 0$ and, assuming vanishing plate thickness, publishes the result without giving a correct derivation. When $\rho = \mu = A$, then $\vartheta = 1/\sqrt{A}$; when A moves toward zero, ϑ goes toward infinity. The term $\kappa \sqrt[4]{\rho}$ equals $\alpha \sqrt{\zeta_a} = \pi/c'_a$, and equals π/c_a' in the shear strength case; here c_a' depends on ϑ only. Thus it may be proved that $\kappa_{kr} \sqrt[4]{\rho}$ is actually constant for a certain ϑ value (say, for $\vartheta = \infty$). With Schmieden's assumption $\rho = \mu$, $\vartheta = \infty$, of course, is synonymous with $\rho = \mu = 0$; that is, with the supposition that bending stiffness D_1 and distortion stiffness D_3 disappear, in this case the shear stress is altogether unstable. To confine the computation of c_a in the shear strength formula to this case alone would be superfluous, because the formula yields $t_{kr} = 0$ anyway. The proof that factor c_a (which is affected by ϑ) arrived at for $\vartheta = \infty$, can be introduced for high, but finite ϑ values, becomes apparent in this report. According to Figure 3a, the error committed (say, for $\vartheta = 30$), does not exceed 3.6% when substituting factor c_a for $\vartheta = \infty$ (instead of $\vartheta = 30$), while with $\vartheta = 1$, the discrepancy is nearly 50%. When the reinforcements are arranged in length and width as Schmieden assumes $(\mu = 0)$, the supposition of vanishing plate thickness equivalent to that of vanishing distortion stiffness, corresponds to the case $\vartheta = \infty$, which (with $\mu = 0$) yields a shear strength different from zero. Schmieden's computed numerical values agree with our data for $\vartheta = \infty$.

then

$$c_a = c_b.$$

To make a stable shear stress at all possible requires a certain bending stiffness $D_2 (> 0)$ although the shear stress by vanishing D_1 or D_3 is stable at the beginning (as long as $t < t_{kr}$).

To enable us to make comparison with Reissner's and Bergmann's latest experiments in which they prove that c_b, when approaching $\vartheta = 0$, is a regular function of $\vartheta^2 = \rho/\mu^2$ and c_a when near $1/\vartheta = 0$ a regular function of $1/\vartheta = \mu/\sqrt{\rho}$, we plotted in Figures 4b and 5b, the c_a factors against ϑ^2. (The c_b factor is the same as in Figure 2b, the only difference being the abscissa.) The dotted secants through the points with abscissas $\vartheta^2 = 0$ and $\vartheta^2 = 0.04$, in Figure 5b, denote the directions of the tangents in the points with the abscissa $\vartheta^2 = 0$. Figure 4b and 5b are alike but for the larger scale of ϑ^2 and its range confined to $0 \leqq \vartheta^2 \leqq 1$.

In similar manner Figure 4a shows the c_a factor plotted against $1/\vartheta$ (like in Figure 2a but for the abscissa), and Figure 5a, c_a plotted against $1/\vartheta$ for $0 \leqq 1/\vartheta \leqq 1$. To approximate the tangent direction in the points with abscissa $1/\vartheta = 0$, the dotted secants are defined by the points with abscissa $1/\vartheta = 0$ and $1/\vartheta = 0.025$ ($\vartheta = \infty$ and $\vartheta = 40$). (The abscissa scale is different from Figure 4a.)

On comparison, we now find that curve $c_b(\vartheta^2)$, in fact from $\rho = 0$ ($D_1 = 0$) to about $\vartheta^2 = \rho/\mu^2 = 0.25$, that is,

$\vartheta = 0.5$, can be substituted by its initial tangent, and that curve $c_a\ (1/\vartheta)$ from $\mu = 0$ $(D_3 = 0)$ to approximately $1/\vartheta = \mu/\sqrt{\rho} = 1$ can be substituted by its initial tangent. As a result c_b, in the neighborhood of $\rho = 0$, can be developed in a power series according to ϑ^2, and c_a, on approaching $\mu = 0$, in a power series according to $1/\vartheta$, as proved analytically by Bergmann and Reissner.

The diagrams can be summarized as follows:

Introducing the constants

c_{ao}	=	8.125	and	15.065
c_{a1}	=	5.64	"	7.685
c_{a2}	=	0.6	"	0.6
c_{bo}	=	11.71	"	18.59
c_{b1}	=	2.155	"	5.86
c_{b2}	=	0.7	"	2.3

we have for pin-jointed and constrained support

$$\frac{t_{kr}\ a^2}{D_2\sqrt[4]{\rho}} = c_a = c_{ao} + c_{a1}\ \frac{1}{\vartheta} - c_{a2}\ \frac{1}{\vartheta^2}$$

(from $\frac{1}{\vartheta} = 0$ to $\frac{1}{\vartheta} = 1$)

$$\frac{t_{kr}\ a^2}{D_2\sqrt{\mu}} = c_b = c_{bo} + c_{b1}\ \vartheta^2 - c_{b2}\ \vartheta^4$$

(from $\vartheta = 0$ to $\vartheta = 1$).

4. The wave length of the elastic surface.- We have already stressed the importance of the tests on the deformations in incipient wrinkling, so as to gain at least an approximate conception of the feasibility of the orthogonal-anisotropic plate (with evenly distributed stiffness).

In this the chief interest centers in the length l of a half wave of the wrinkle measured in the direction of the x-axis, which must be greater than the spacing of the stiffeners, or the assumption of a mean value for the bending stiffness D_2 is no longer valid. The length of the half-wave of the elastic surface (measured along the plate length) which begins to form under critical shear can be computed for the ideal orthogonal-anisotropic plate with one of the two equations:

$$l_{kr} = c_a' \, a \sqrt[4]{\frac{D_1}{D_2}} = c_a' \, a \sqrt[4]{\rho} \tag{4a}$$

$$l_{kr} = c_b' \, a \sqrt{\frac{D_3}{D_2}} = c_b' \, a \sqrt{\mu} \tag{4b}$$

The absolute factors c_a' and c_b' are, like c_a and c_b, dependent on ϑ (formula 3) and can be read from Figures 6a and 6b. (Factor c_a' is used to determine (for $\vartheta > 1$) the half-wave length forming on the elastic surface at wrinkling ($l_{kr} = c_a' \, a\sqrt[4]{\rho}$), Figure 6a; and c_b' (for $\vartheta < 1$) to determine the half-wave length at wrinkling ($l_{kr} = c_b' \, a\sqrt{\mu}$), Figure 6b.) When $\vartheta > 1$, equation (4a), when $\vartheta < 1$, equation (4b) should be used.

The approximate formulas for the wave lengths with constants

$c_a'_o = 2.05$ and 1.38, $c_b'_o = 1.92$ and 1.16

$c_a'_1 = 0.44$ " 0.28, $c_b'_1 = 0.57$ " 0.9

$c_b'_2 = 0$ " 0.4

are

$$c_a' = c_a'_o + c_a' \frac{1}{\vartheta} \qquad \text{(from } \frac{1}{\vartheta} = 0 \text{ to } \frac{1}{\vartheta} = 1\text{)}$$

$$c_b' = c_b'_o + c_b'_1 \vartheta^2 - c_b'_2 \vartheta^4 \qquad \text{(" } \vartheta = 0 \text{ " } \vartheta = 1\text{)}.$$

for elastically and rigidly constrained support.

5. Example.- A long, flat, rectangular duralumin plate of $2a = 100$ cm width and $\delta = 0.05$ cm thickness, like the cross section shown in Figure 7 (along x-axis, plate length) is equipped with riveted angle plates which run parallel to the y-axis (plate width direction). The even spacing (distance at center) of the stiffeners is $d = 4.0$ cm. No stiffeners are provided in the x-axis.

We disregard the transverse elongation for the present, so that Poisson's ratio becomes $\nu = 0$; of course, this does not hold good when the shear modulus of the material is $G = \frac{1}{2} E$; E = Young's modulus.

Owing to the difficulty of correct interpretation of the elastic edge restraint, it is no more than a rough calculation, so that our simplifying assumption is justifiable. Moreover, the cross stress in a reinforced plate is decidedly less effective than in a strictly homogeneous plate.

The angle plates have no appreciable effect on bending

stiffness D_1, so that we can substitute that of the nonreinforced plate, which, ignoring the transverse elongation, yields

$$D_1 = \frac{E\,\delta^3}{12}$$

$$= \frac{7 \times 10^5 \times 0.05^3}{12}$$

$$= 7 \times 1.04 \text{ kg cm}$$

$E = 700{,}000 \text{ kg/cm}^2$.

The stiffeners have likewise no marked effect on the distortion stiffness, so that (omitting ν_x and ν_y):

$$D_3 = 2(GJ)_{xy}$$

$$= \frac{E\,\delta^3}{12}$$

$$= 7 \times 1.04 \text{ kg cm}$$

The cross-sectional inertia moment of four angle plates with respect to the x-axis is

$$J = 0.665 \text{ cm}^4,$$

so that the mean bending stiffness D_2 becomes

$$D_2 = \frac{E\,J}{d} + \frac{E\,\delta^3}{12}$$

$$= \frac{7 \times 10^5 \times 0.665}{4} + 7 \times 1.04$$

$$= 7 \times 1664 \text{ kg cm}$$

According to (3)

$$\vartheta = \frac{7 \times \sqrt{1.04 \times 1664}}{7 \times 1.04}$$

$$= 40.$$

The figures, 2a and 2b, yield the corresponding value:

$$c_{af} = 8.25 \quad \text{(free support)},$$

and

$$c_{ae} = 15.25 \quad \text{(rigid edge restraint)},$$

so the shear strength computed with (1a) becomes:

$$t_{kr\,f} = 8.25 \times \frac{7 \times \sqrt[4]{1.04 \times 1664^3}}{50^2},$$

$$= 6.1 \text{ kg/cm} \quad \text{(free support)},$$

and

$$t_{kr\,e} = 15.25 \times \frac{7 \times \sqrt{1.04 \times 1664^3}}{50^2},$$

$$= 11.25 \text{ kg/cm} \quad \text{(rigid restraint)}.$$

To determine the distance l_{kr} of the junction lines on the elastic surface, we resort to the factors given in Figures 6a and 6b. For $\vartheta = 40$, we substitute the figures for $\vartheta = \infty$:

$$c_a'_f = 2.05$$

and

$$c_a'_e = 1.38$$

where, according to (4a), the half-wave length is defined as

$$l_{kr\,f} = 2.05 \times 50 \sqrt[4]{\frac{1.04}{1664}}$$

$$= 16.2 \text{ cm}$$

$$l_{kr\,e} = 1.38 \times 50 \sqrt[4]{\frac{1.04}{1664}}$$

$$= 10.9 \text{ cm}.$$

In the present case the half-wave length exceeds the center distance d of the stiffeners; moreover, the distribution of the reinforcements is comparably uniform within length l, so

that the calculated shear strength should be quite accurate.

In a subsequent section (10, page 49) (Figures 15a and 15b), we show that a slight deviation (increase or decrease) in half-wave length - in a homogeneous orthogonal-anisotropic plate - presupposes an increase in shear load only slightly lower than that of the shear strength. A certain discrepancy from the figure given by formula (4) always will exist, unless the reinforcements are distributed perfectly evenly and with vanishingly small spacing.

Naturally, we must not conclude herefrom that the shear strength computed by equation (1) would always be a little too low. The local reinforcements affect the position of the junction lines (at variance with the approximate calculation) so that the reinforced points on the plate are subjected to lower form changes than the approximation calls for, and the whole work of deflection at wrinkling, and thereby the shear strength, is perhaps lower than the calculation warrants.

In order to define the influence of the reinforcing plates on the shear strength we examine the nonreinforced 0.5 mm thick duralumin plate (plate strip without angle plate, $2a = 100$ cm). Again disregarding the transverse elongation, the plate stiffness is written as

$$D_1 = D_2 = D_3 = \frac{E\,\delta^3}{12}$$

$$= 7 \times 1.04 \text{ kg cm}$$

Including the transverse elongation, we have instead of $E\,\delta^3/12$,

for D (D_1, D_2, D_3):

$$D = \frac{E \delta^3}{12 (1 - \nu^2)} ;$$

The D value now is multiplied by a factor

$$c_\nu = \frac{1}{1 - \nu^2}$$

Poisson's ratio ν for metals is

$$\nu = 0.25 \text{ to } 0.3.$$

This corresponds to factor

$$c_\nu = 1.07 \text{ to } 1.10.$$

With $c_\nu = 1.07$ for duralumin, we obtain*

$$D = 1.07 \times 7 \times 1.04 = 7.8 \text{ kg cm.}$$

Since $\vartheta = 1$, we have

$$t_{kr\,f} = 13.165 \times \frac{7.8}{50^2} = 0.041 \text{ kg/cm} \quad \text{(freely supported)}$$

$$t_{kr\,e} = 22.15 \times \frac{7.8}{50^2} = 0.069 \text{ kg/cm} \quad \text{(rigidly restrained)}$$

$$\tau_{kr\,f} = \frac{0.041}{0.05} = 0.82 \text{ kg/cm}$$

$$\tau_{kr\,e} = \frac{0.069}{0.05} = 1.38 \text{ kg/cm}$$

$$l_{kr\,f} = 2.49 \times 50 \sqrt[4]{\frac{7.8}{7.8}} = 124.5 \text{ cm}$$

$$l_{kr\,e} = 1.66 \times 50 = 83.0 \text{ cm.}$$

*Bending and distortion tests on duralumin plates yielded as high as $\nu = 0.24$. (Compare Z. f. Tech. Physik, Vol. 8, 1927, pp. 355-359: M. Bergstrasser, "Determination of the Two Elastic Constants in Platelike Bodies.") The equivalent of $\nu = 0.24$ would be $c_\nu = 1.06$.

For $\nu = 0$, the figures for t_{kr} and τ_{kr} would be 7% lower; l_{kr} would remain unchanged.

The critical shear stress of the nonreinforced strip lying between the angle plates can be calculated in the same manner (Fig. 7). The half-width of these strips is less than 1 cm.

Calculating without restraint, we obtain a critical shear stress which in any case is higher than

$$t_{kr} = 13.165 \times \frac{7.8}{1.0^2}$$
$$= 103 \text{ kg/cm}$$

As is to be expected, this figure is far above that found for the whole reinforced plate.

The conformity of very thin isotropic homogeneous plates with our assumptions set up in the development of the formulas - plate thickness small compared to length and width, and small elastic deflection relative to plate thickness - may lead one to conclude that the computed elastic surface would appear particularly well in tests with very thin plates. This, however, is not always true, because such plates cannot be manufactured absolutely flat and show small bulges which, owing to the thinness of the material must be taken into consideration.

III. Investigation

6. The differential equation of the elastic surface of an orthogonal-anisotropic plate.- Let

p = load per unit of plate area acting perpendicularly to the median plane;

M_y and M_x = bending moments per unit of length acting on areas of intersection $\delta\, dx$ and $\delta\, dy$;

$H_{xy} = H_{yx} = H$ = shear moments per unit of length acting on the areas of intersection.

The equation of equilibrium between load p and moments M_x, M_y, and H then reads:

$$\frac{\partial^2 M_x}{\partial x^2} + \frac{2\,\partial^2 H}{\partial x\, \partial y} + \frac{\partial^2 M_y}{\partial y^2} + p = 0 \qquad (5)$$

No assumptions as to the elastic properties of the plate were made, and the equation applies equally to a plate with any elastic property or with any elongation in plate area.

Each of these moments, M_x, M_y, and H induces certain elastic deformations, but of which only the deformations w (in the direction of the z axis, positive, downward) hold any particular interest for us. With only a constant bending moment M_x (that is, $M_y = H = 0$) acting in an arbitrarily long part of the plate, the result - when all points of the plate are identical in elastic property, i.e., the plate is homogeneous - is

1) a constant curvature (about y-axis) along x-axis;

2) a certain (lower) curvature (about x-axis) in the y-direction, due to the transverse elongation. So in order to describe

this form change, we naturally must know the two necessary quantities on which the elastic properties of the material depend (constant in homogeneous materials). This applies to moment M_y also. With only H (that is, $M_x = M_y = 0$), active, a distortion results. H acts on all four intersections (δ dx and δ dy) of the assumedly cut-out plate elements, which, to describe this attitude of deformation, requires only one elastic quantity (a constant in homogeneous material).

The special (orthogonal) anisotropy of the plate is inferred from the absence of distortion by the bending moments M_x or M_y, and from the absence of deflection by distortion moment H with respect to the x, y axes. Owing to the limitation to small deflections w, the ensuing small quantities are negligible and the curvature is expressed as $\frac{\partial^2 w}{\partial x^2}$ and $\frac{\partial^2 w}{\partial y^2}$, and the distortion as $\frac{\partial^2 w}{\partial x \partial y}$.

Now the described elastic properties of the orthogonal-anisotropic plate can be written as

$$\left.\begin{aligned} \frac{\partial^2 w}{\partial x^2} &= -\frac{1}{(EJ)_x} M_x + \frac{\nu_y}{(EJ)_y} M_y \\ \frac{\partial^2 w}{\partial y^2} &= -\frac{1}{(EJ)_y} M_y + \frac{\nu_x}{(EJ)_x} M_x \\ \frac{\partial^2 w}{\partial x \partial y} &= -\frac{1}{2\,(GJ)_{xy}} H \end{aligned}\right\} \qquad (6)$$

with ν_x and ν_y as certain ideal Poisson's ratios. Resolving these equations according to M_x, M_y and H, we have

$$\left.\begin{aligned} M_x &= -\frac{(EJ)_x}{1-\nu_x\,\nu_y}\left(\frac{\partial^2 w}{\partial x^2}+\nu_y\frac{\partial^2 w}{\partial y^2}\right) \\ M_y &= -\frac{(EJ)_y}{1-\nu_x\,\nu_y}\left(\frac{\partial^2 w}{\partial y^2}+\nu_x\frac{\partial^2 w}{\partial x^2}\right) \\ H &= -2\,(GJ)_{xy}\frac{\partial^2 w}{\partial x\,\partial y} \end{aligned}\right\} \qquad (7)$$

The five elastic quantities $(EJ)_x$, $(EJ)_y$, $(GJ)_{xy}$, ν_x and ν_y now are defined by formulas (6) and (7); the elastic quantities need not even be constants; they might also be functions of the locus (nonhomogeneous plate). Accordingly, these elastic quantities must be defined by experiments in bending and distortion in which only one constant bending and distortion moment is active. Poisson's ratio ν_x and ν_y is generally low enough to be set at zero for the conventional plate reinforcements. Beginning, as in the case of the flat, homogeneous plate, with simple load cases (tension and shear loading) and deriving equations (6) by applying some known theorem (Hooke, Bernoulli), the five elastic quantities can be determined from the tension and shear load attitudes. But inasmuch as this does not enter into the question in the majority of the systems considered here, we assume these elastic quantities defined by (6) and (7).

The work of form change of an orthogonal-anisotropic plate, loaded with moments M_x and M_y is unaffected by the sequence in which M_x and M_y are used, and the elastic quantities yield, according to Maxwell and Betti, the following relation,

$$\nu_y (EJ)_x = \nu_x (EJ)_y$$

Thus the orthogonal anisotropy of a thin plate is characterized by four elastic quantities, the case of general anisotropy of a thin plate by six, and the three-dimensional body by 21 quantities.

Putting, briefly,

$$\left.\begin{aligned} D_1 &= \frac{(EJ)_x}{1 - \nu_x \nu_y} \\ D_2 &= \frac{(EJ)_y}{1 - \nu_x \nu_y} \\ 2 D_3 &= \nu_x \frac{(EJ)_y}{1 - \nu_x \nu_y} + \nu_y \frac{(EJ)_x}{1 - \nu_x \nu_y} + 4 (GJ)_{xy} \end{aligned}\right\} \qquad (8)$$

and inserting formulas (7) in formula (5) the differential equation of the elastic surface of a thin orthogonal-anisotropic plate reads

$$D_1 \frac{\partial^4 W}{\partial x^4} + 2 D_3 \frac{\partial^4 W}{\partial x^2 \partial y^2} + D_2 \frac{\partial^4 W}{\partial y^4} - p = 0 \qquad (9)$$

7. Stability equation, edge equations and theorem for resolving the differential equation.- Subjecting the edges of an elastic, orthogonal-anisotropic strip of infinite length and of 2a width to an evenly distributed shear t, produces at first a pure shear stress attitude in the plate, but as soon as t reaches a certain magnitude, the plate begins to buckle. This limiting case of the stability is given for the lowest load

t (t_{kr}), and equation (9) is complied with when we set

$$- p = + 2t \frac{\partial^2 w}{\partial x \partial y},$$

and (9) becomes

$$D_1 \frac{\partial^4 w}{\partial x^4} + 2D_3 \frac{\partial^4 w}{\partial x^2 \partial y^2} + D_2 \frac{\partial^4 w}{\partial y^4} + 2t \frac{\partial^2 w}{\partial x \partial y} = 0 \qquad (10)$$

Since the strip is of infinite length it is necessary that the solution be periodic in the longitudinal direction (x). According to Southwell and Skan, we wrire

$$w = e^{i\kappa \frac{x}{a}} \sum_{r=2}^{r=4} C_r \, e^{i\lambda_r \frac{y}{a}} \qquad (11)$$

where κ is to be real, and the quantities λ real or complex.

This equation, written in (10) then yields

$$e^{i\kappa \frac{x}{a}} \sum_{r=1}^{r=4} C_r \, e^{i\lambda_r \frac{y}{a}} \left[D_1 \frac{\kappa^4}{a^4} + 2 D_3 \frac{\kappa^2}{a^2} \frac{\lambda_r^2}{a^2} + \right.$$

$$\left. + D_2 \frac{\lambda_r^4}{a^4} - 2t \frac{\kappa}{a} \frac{\lambda_r}{a} \right] = 0$$

Now we add the real quantities (Compare formula (2))

$$\mu = \frac{D_3}{D_2}, \quad \rho = \frac{D_1}{D_2} \quad \text{and} \quad \tau_1 = \frac{t \, a^2}{D_2}$$

and we arrive at the characteristic equation with the unknown factor λ:

$$\lambda^4 + 2 \mu \kappa^2 \lambda^2 - 2 \tau_1 \kappa \lambda + \rho \kappa^4 = 0 \qquad (12)$$

With λ_1, λ_2, λ_3, and λ_4 as the roots of this formula, we have

$$(\lambda - \lambda_1)(\lambda - \lambda_2)(\lambda - \lambda_3)(\lambda - \lambda_4) = 0 \qquad (12a)$$

Since the term with λ^3 does not appear in (12), as a comparison of the coefficients in (12) and (12a) shows, the four roots must comply with

$$\lambda_1 + \lambda_2 + \lambda_3 + \lambda_4 = 0,$$

and we express them as

$$\left.\begin{aligned} \lambda_1 &= \alpha\,(+\,1 + n) \\ \lambda_2 &= \alpha\,(+\,1 - n) \\ \lambda_3 &= \alpha\,(-\,1 + m) \\ \lambda_4 &= \alpha\,(-\,1 - m) \end{aligned}\right\} \tag{13}$$

The coefficients in (12) ($+ 2\,\mu\,\kappa^2$, $- 2\,\tau_1\,\kappa$ and $+\,\rho\,\kappa^4$) are real; if this equation has a complex instead of real root, the conjugate-complex number is a root also. The result is that m and n are either real or purely imaginary (that is, in no case somplex), and α always real.

A comparison of the factors in (12) with those in (12a) yields for λ, that is, for α, m and n

$$\left.\begin{aligned} &\text{a)}\quad \alpha^2\,(-\,2 - n^2 - m^2) = 2\,\mu\,\kappa^2 = 2\,\frac{D_3}{D_2}\,\kappa^2 \\ &\text{b)}\quad \alpha^4\,(1 - n^2)\,(1 - m^2) = \rho\,\kappa^4 = \frac{D_1}{D_2}\,\kappa^4 \\ &\text{c)}\quad \alpha^3\,(n^2 - m^2) = \tau_1\,\kappa = \frac{t\,a^2}{D_2}\,\kappa \end{aligned}\right\} \tag{14}$$

and further relations between α, m, and n furnish the edge equations.

The plate strip is supported on the edges $y = + a$ and $y = - a$, and we assume that there is no deflection on these

edges. Now, the first two equations are

$$\left.\begin{aligned} a) \quad (w)_{y=+a} &= 0 \\ b) \quad (w)_{y=-a} &= 0 \end{aligned}\right\} \tag{15}$$

This conforms to the supposition of bending-resistant edge supports.*

Moreover, we must determine the effect of the type of support on the tangent slope $\frac{\partial w}{\partial y}$ of the elastic surface at the edges. If the support is on knife-edges the plate is not pre-

*The inclusion of bending of the longitudinal support could be accomplished by means of one of the following equations for the elastic line of the edge support with $(E'J_b)$ bending stiffness, namely

$$(E' J_b) \left(\frac{\partial^2 w}{\partial x^2}\right)_{y=\pm a} = - M_b$$

or

$$(E' J_b) \left(\frac{\partial^4 w}{\partial x^4}\right)_{y=\pm a} = p_1$$

In the first formula the bending moment at point x of the edge support is calculated as the sum of all turning moments of the cross stress Q_y and of the turning moment H of the plate at the cut-off part; that is, when the girder is nowhere supported:

$$M_b = \int_{-\infty}^{x} [Q_y (x - \xi) + H] \, d\xi$$

In the second equation the loading p_1 per unit of length, comprises the cross stress Q_y and the derivative of H, that is:

$$p_1 = \left(Q_y + \frac{\partial H}{\partial x}\right)_{y=\pm a}$$

The edge girder need no support because, due to the periodic character of the solution, the edge stresses are in equilibrium. If, however, a support is provided, the latter must be evenly spaced (l) so as to conform to the periodic solution (equation (11)) and, in addition, the solution is generally narrowed because of the added formula,

$$(w)_{y=\pm a,\ x=n l} = 0$$

vented from such a slope of its elastic surface. But as a rule, the plate is so fastened to the edge support that, by perfect attachment, this support distorts to an amount equivalent to angle $\frac{\partial w}{\partial y}$ of the elastic surface on the bearing. If the edge support offers an elastic resistance against this distortion, it produces bending moments M_y in the plate and distortion moments (per unit length) in the edge support of the same size as the plate bending moments, and the restraint is elastic. Now it may be inferred that the increase in distortion angle (per unit length of support axis, or, of the edge line) of the edge support is at every point proportional to the (inside) turning moment of the edge support. This corresponds, strictly speaking, to a support of constant, round cross section with uniform distribution of the turning moments over the cross sectional periphery. But in first approximation it could equally be applied to other than round cross sections.

At the edge $y = + a$ the distortion angle at any point is

$$\delta = \left(\frac{\partial w}{\partial y}\right)_{y=+a}$$

and the increase in distortion angle per unit length is

$$\frac{d\delta}{dx} = \left(\frac{\partial^2 w}{\partial x \partial y}\right)_{y=+a}$$

the distortion load m_d applied to the support per unit length now equals the bending moment $(M_y)_{y=+a}$ of the plate; hence, according to (7) and (8):

$$m_d = - D_2 \left(\frac{\partial^2 w}{\partial y^2}\right)_{y=+a} - \nu_x D_2 \left(\frac{\partial^2 w}{\partial x^2}\right)_{y=+a}$$

The inside distortion moment acting at point x is found by integrating over the distortion load m_d, assuming the edge support to be unprotected against distortion.

We write:

$$M_d = - \int_{-\infty}^{x} \left[D_2 \left(\frac{\partial^2 w}{\partial y^2}\right)_{y=+a} + \nu_x D_2 \left(\frac{\partial^2 w}{\partial x^2}\right)_{y=+a}\right] d x)^*$$

With $(G'J_d)$ as distortion resistance, we have

$$\frac{d\delta}{dx} = \frac{M_d}{(G' J_d)} ,$$

and, by inserting the corresponding values

$$\left(\frac{\partial^2 w}{\partial x \partial y}\right)_{y=+a} = - \frac{1}{(G' J_d)} \int_{-\infty}^{x} \left[D_2 \left(\frac{\partial^2 w}{\partial y^2}\right)_{y=+a} + \nu_x D_2 \left(\frac{\partial^2 w}{\partial x^2}\right)_{y=+a}\right] d x \qquad (15c)$$

For edge $y = - a$ the conformal equation (since distortion $\frac{\partial^2 w}{\partial x \partial y}$ has a corresponding distortion moment $m_d = - (M_y)_{y=-a}$ is

*The integration can be avoided, as in the preceding footnote, by using another (equivalent) form of torsion balance of the edge support, namely,

$$(G' J_d) \frac{d^2 \delta}{dx^2} = - m_d$$

instead as above

$$(G' J_d) \frac{d\delta}{dx} = M_d = - \int_{-\infty}^{x} m_d \, dx$$

$$\left(\frac{\partial^2 w}{\partial x\, \partial y}\right)_{y=-a} = + \frac{1}{(G' J_d)} \int_{-\infty}^{x} \left[D_2 \left(\frac{\partial^2 w}{\partial y^2}\right)_{y=-a} + \right.$$

$$\left. + \nu_x D_2 \left(\frac{\partial^2 w}{\partial x^2}\right)_{y=-a} \right] d x \qquad (15d)$$

Now we insert (11) in (15a) to (15d) and have:

$$(a,b) \quad e^{i\kappa \frac{x}{a}} \sum_{r=1}^{r=4} C_r\, e^{\pm i \lambda_r} = 0$$

$$(c,d) \quad \frac{\kappa}{a^2}\, e^{i\kappa \frac{x}{a}} \sum_{r=1}^{r=4} C_r\, \lambda_r\, e^{\pm i \lambda_r}$$

$$= \pm \frac{1}{(G' J_d)\, i\, \kappa\, a}\, e^{i\kappa \frac{x}{a}} \left[D_2 \sum_{r=1}^{r=4} C_r\, \lambda_r^2\, e^{\pm i \lambda_r} + \right.$$

$$\left. + \nu_x D_2\, \kappa^2 \sum_{r=1}^{r=4} C_r\, e^{\pm i \lambda_r} \right] .$$

In the terms with double signs, the upper sign (equations a and c) is valid once only in each equation, and then the lower sign for equations b and d. The last term in (c,d) disappears according to equation (a,b). The relation for $e^{i\lambda_r}$ is

$$e^{\pm i \lambda_r} = \cos \lambda_r \pm i \sin \lambda_r$$

and we abbreviate

$$\epsilon = \frac{D_2\, a}{(G' J_d)\, \kappa^2}$$

Now the equations (a,b) and (c,d) become:

$$(a,b) \ldots\ \sum_{r=1}^{r=4} C_r \cos \lambda_r \pm i \sum_{r=1}^{r=4} C_r \sin \lambda_r = 0$$

$$(c,d) \ldots \left(\sum_{r=1}^{r=4} C_r\, \lambda_r \cos \lambda_r + \epsilon \sum_{r=1}^{r=4} C_r\, \lambda_r^2 \sin \lambda_r \right)$$

$$\pm i \left(\sum_{r=1}^{r=4} C_r\, \lambda_r \sin \lambda_r - \epsilon \sum_{r=1}^{r=4} C_r \lambda_r^2 \cos \lambda_r \right) = 0$$

Setting the real and the imaginary parts of this equation to zero, the four-edge equations now read

$$\left.\begin{aligned}
&\text{a)}\quad \sum_{r=1}^{r=4} C_r \cos \lambda_r = 0 \\
&\text{b)}\quad \sum_{r=1}^{r=4} C_r \sin \lambda_r = 0 \\
&\text{c)}\quad \sum_{r=1}^{r=4} C_r \lambda_r \cos \lambda_r + \epsilon \sum_{r=} C_r \lambda_r^2 \sin \lambda_r = 0 \\
&\text{d)}\quad \sum_{r=1}^{r=4} C_r \lambda_r \sin \lambda_r - \epsilon \sum_{r=} C_r \lambda_r^2 \cos \lambda_r = 0
\end{aligned}\right\} \qquad (16)$$

These are four homogeneous equations with the unknown C factors. To assure nondisappearing C values, the determinant of the denominator must disappear. This yields a transcendent equation with the four λ roots; by introducing (13) we establish a relation between α, n, m, and ϵ.

ϵ depends on the form of the edge supports and may, according to $(G' J_d)$ assume any value between zero and infinity. To simplify the calculation, we use only these two limiting values of ϵ in the subsequent examination.

For

$$\epsilon = 0,$$

it corresponds to an infinitely high $(G' J_d)$, value, that is, an edge rigid in distortion; this is the case of rigid restraint (case "e"), where the angle of tangent slope $\frac{\partial w}{\partial y}$ of the elastic surface equals zero at the edge.

Now we divide (16c) and (16d) by ϵ, and make

$$\frac{1}{\epsilon} = 0, \quad \text{that is,} \quad \epsilon = \infty,$$

which corresponds to the knife-edge support (free support, case "f") of the plate edge, and where bending moment $(M_y)_{y=\pm a}$ disappears.

When we insert the given values, and determinant of the denominator becomes zero, the relations between α, n, and m, for cases "f" and "e" are:

$$\left.\begin{aligned} &\text{f)}\quad 8\,n\,m\,[\cos 2\,n\,\alpha \cos 2\,m\,\alpha - \cos 4\,\alpha] \\ &\quad -[4\,(n^2 + m^2) - (n^2 - m^2)^2]\sin 2\,n\,\alpha \sin 2\,m\,\alpha = 0 \\ &\qquad\qquad\qquad\qquad\qquad\qquad\qquad\qquad \text{(by free support)} \\ &\text{e)}\quad 2\,n\,m\,[\cos 2\,n\,\alpha \cos 2\,m\,\alpha - \cos 4\,\alpha] \\ &\quad -[4 - n^2 - m^2]\sin 2\,n\,\alpha \sin 2\,m\,\alpha = 0 \\ &\qquad\qquad\qquad\qquad\qquad\qquad\qquad\qquad \text{(by rigid restraint)} \end{aligned}\right\} \quad (17)$$

8. The critical shear stress.- The equation (14) combined with one of (17) yield the relations between D_1, D_2, D_3, a and that shear stress t, at which the pure shear stress ceases to present a stable attitude of equilibrium, but where the equilibrium equations yield a possible state of deflection conformably to equation (11). Hereby it is assumed that the stresses consistent with this attitude do not exceed the proportional elastic limit.

The four equations - (14a, b, c), (17f) and (17e), respectively, contain five unknown factors: κ, α, n, m, and t. The κ value determines, in accordance with equation (11), the wave length of the elastic surface in the direction of axis x.

In a definite system with definite D_1, D_2, D_3, and a, we

may at first assume an arbitrary wave length, or a suitable κ, and then determine the respective t from the four equations. The desired shear strength t_{kr} is the lowest t value at which the plate commences to wrinkle, or in other words, where a function w (equation 11) different from zero, prevails.

To extend the applicability of the systems considered here (for arbitrary D_1, D_2, D_3, and a) we transform the equations. We introduce in (14) the factor ϑ for the orthogonal-anisotropic plate defined from equation (3)

$$\vartheta = \frac{\sqrt{D_1 \; D_2}}{D_3} = \frac{\sqrt{\rho}}{\mu}$$

which may assume any real value from zero to infinity. Then we introduce the parameters

$$\left.\begin{aligned} &\text{a)} \quad \zeta_a = \sqrt{\frac{D_1}{D_2}} \left(\frac{\kappa}{\alpha}\right)^2 = \sqrt{\rho} \left(\frac{\kappa}{\alpha}\right)^2 \\ &\text{b)} \quad \zeta_b = \frac{D_3}{D_2} \left(\frac{\kappa}{\alpha}\right)^2 = \mu \left(\frac{\kappa}{\alpha}\right)^2 \\ &\qquad\quad = \frac{\zeta_a}{\vartheta} \end{aligned}\right\} \tag{18}$$

Now we divide (17) into a transcendent function φ equivalent for cases f and e, which contains α, m, and n, and into an algebraic function ψ different for cases f and e, and which contains n and m only.

The result is

$$\left.\begin{aligned}
&\text{a)} \quad -1 - \frac{n^2 + m^2}{2} = \frac{1}{\vartheta}\,\zeta_a \quad \text{and} \quad = \zeta_b \\
&\text{b)} \quad (1 - n^2)(1 - m^2) = \zeta_a^2 \quad \text{and} \quad = \vartheta^2\,\zeta_b^2 \\
&\text{c)} \qquad t = \frac{\sqrt[4]{D_1\,D_2^{\,3}}}{a^2} \times \frac{\alpha^2\,(n^2 - m^2)}{\sqrt{\zeta_a}} \\
&\qquad\qquad \text{and} \quad = \frac{D_2\,D_3}{a^2} \times \frac{\alpha^2\,(n^2 - m^2)}{\sqrt{\zeta_b}}
\end{aligned}\right\} \tag{19}$$

With Bergmann and Reissner designations (19c) becomes:

$$\frac{t\,a^2}{D_2} = \frac{\alpha^3\,(n^2 - m^2)}{\kappa} = \sqrt[4]{\rho}\,\frac{\alpha^2\,(n^2 - m^2)}{\sqrt{\zeta_a}} \quad \text{and} \quad = \sqrt{\mu}\,\frac{\alpha^2\,(n^2 - m^2)}{\sqrt{\zeta_b}}$$

$$\left.\begin{aligned}
&\text{f)} \quad \varphi = \psi_f \quad \text{(by free support)}, \\
&\text{e)} \quad \varphi = \psi_e \quad \text{(by rigid restraint)};
\end{aligned}\right\} \tag{20}$$

it denotes

$$\varphi = \frac{\sin 2\,n\,\alpha \sin 2\,m\,\alpha}{\cos 2\,n\,\alpha \cos 2\,m\,\alpha - \cos 4\,\alpha} = \omega \tan 2\,n\,\alpha \tan 2\,m\,\alpha$$

if we make

$$\omega = \frac{1}{1 - \dfrac{\cos 4\,\alpha}{\cos 2\,n\,\alpha \cos 2\,m\,\alpha}}$$

and

$$\psi_f = \frac{8\,n\,m}{4\,(n^2 + m^2) - (n^2 - m^2)^2}$$

$$\psi_e = \frac{2\,n\,m}{4 - (n^2 + m^2)}\,.$$

This is simplified with

$$\left.\begin{aligned} \text{a)}\quad C_a &= \frac{\alpha^2 (n^2 - m^2)}{\sqrt{\zeta_a}} \\ \text{b)}\quad C_b &= \frac{\alpha^2 (n - m^2)}{\sqrt{\zeta_b}} \end{aligned}\right\} \qquad (21)$$

$$= C_a \sqrt{\vartheta} \quad \text{(See equation 18b)},$$

and the shear strength t of equation (19c) now yields

$$\text{a)}\quad t = C_a \frac{\sqrt[4]{D_1 D_2^3}}{a^2} \qquad \frac{t a^2}{D_2} = C_a \sqrt[4]{\rho}$$

$$\text{b)}\quad t = C_b \frac{\sqrt{D_2 D_3}}{a^2} \qquad \frac{t a^2}{D_2} = C_b \sqrt{\mu}$$

For the case that t represents the lowest value actually obtainable, i.e., shear strength t_{kr}, we have

$$\text{a)}\quad t_{kr} = c_a \frac{\sqrt[4]{D_1 D_2^3}}{a^2} \qquad \frac{t_{kr} a^2}{D_2} = c_a \sqrt[4]{\rho}$$

$$\text{b)}\quad t_{kr} = c_b \frac{\sqrt{D_2 D_3}}{a^2} \qquad \frac{t_{kr} a^2}{D_2} = c_b \sqrt{\mu}$$

when

and

$$\left.\begin{aligned} \text{a)}\quad c_a &= \left[\frac{\alpha^2 (n^2 - m^2)}{\sqrt{\zeta_a}}\right]_{min} \\ \text{b)}\quad c_b &= \left[\frac{\alpha^2 (n^2 - m^2)}{\sqrt{\zeta_b}}\right]_{min} \end{aligned}\right\} \qquad (21')$$

These are values which, as we shall show, may be represented as simple functions of ϑ.

Now we proceed as follows: We determine n and m as terms of ϑ and of ζ_a or ζ_b, conformally to (19a) and (19b); then we compute the corresponding α from (20f) or (20e), and C_a and C_b from (21). C_a and C_b assume, as ζ_a and ζ_b func-

tions, certain minimums for each ϑ (value). These minimums represent the desired coefficients c_a and c_b.

Now we ascertain whether C_a and C_b and thereby t as functions of ϑ and ζ_a (and ζ_b) are so formed that these functions represent a solution of equation (11) when ϑ assumes any value between zero and infinity; then we must find the range of ζ_a and ζ_b as functions and their minimum value.

We begin with the partial functions which comprise function C_a (and C_b) - equations (21a) and (21b).

From (19a) and (19b) we calculate n and m as well as $(n^2 + m^2)$, $(n^2 - m^2)$, and n m:

$$\left.\begin{aligned}
\frac{n^2 + m^2}{2} &= -\left(1 + \frac{\zeta_a}{\vartheta}\right) \\
\text{and} \qquad &= -(1 + \zeta_b) \\
\frac{n^2 - m^2}{2} &= +\sqrt{\left(2 + \frac{\zeta_a}{\vartheta}\right)^2 - \zeta_a^2} \\
\text{and} \qquad &= +\sqrt{(2 + \zeta_b)^2 - \vartheta^2\,\zeta_b^2} \\
n &= \pm\sqrt{\frac{n^2 + m^2}{2} + \frac{n^2 - m^2}{2}} \\
&= \pm\sqrt{-\left(1 + \frac{\zeta_a}{\vartheta}\right) + \sqrt{\left(2 + \frac{\zeta_a}{\vartheta}\right)^2 - \zeta_a^2}} \\
\text{and} \qquad &= \pm\sqrt{-(1 + \zeta_b) + \sqrt{(2 + \zeta_b)^2 - \vartheta^2\,\zeta_b^2}} \\
m &= \pm\sqrt{\frac{n^2 + m^2}{2} - \frac{n^2 - m^2}{2}} \\
&= \pm\sqrt{-\left(1 + \frac{\zeta_a}{\vartheta}\right) - \sqrt{\left(2 + \frac{\zeta_a}{\vartheta}\right)^2 - \zeta_a^2}}
\end{aligned}\right\} \qquad (22)$$

$$\left.\begin{aligned} \text{and} \qquad &= \pm\sqrt{-(1+\zeta_b) - \sqrt{(2+\zeta_b) - \vartheta^2\,\zeta_b^2}} \\ n\,m \qquad &= \sqrt{\left(\frac{n^2+m^2}{2}\right)^2 - \left(\frac{n^2-m^2}{2}\right)^2} \\ &= \sqrt{\zeta_a^2 - \frac{2\,\zeta_a}{\vartheta} - 3} \\ \text{and} \qquad &= \sqrt{\vartheta^2\,\zeta_b^2 - 2\,\zeta_b - 3} \end{aligned}\right\}$$

According to assumption (equations 11 and 13) κ and α, as well as ϑ (equation 13) are real; thus it follows from (18) that ζ_a and ζ_b are always real and positive. But, according to (22), $(n^2 + m^2)$ are always real (and negative). So n and m are either real or purely imaginary, but never complex (Compare equation 13); this is feasible only when $(n^2 - m^2)$ is real also; or, in other words, (Compare equation 22) when

$$\left(2 + \frac{\zeta_a}{\vartheta}\right)^2 \geqq \zeta_a^2.$$

Then we can write

$$2 + \frac{\zeta_a}{\vartheta} \geqq \zeta_a$$

For $\vartheta \leqq 1$ this equation is complied with for every positiva ζ_a, while $\vartheta > 1$ yields

$$\left.\begin{aligned} &\zeta_a \leqq \frac{2\,\vartheta}{\vartheta - 1}\left(= \frac{2}{1 - \frac{1}{\vartheta}}\right) \\ \text{and} \qquad &\zeta_b \leqq \frac{2}{\vartheta - 1} \end{aligned}\right\} \quad (\text{for } \vartheta > 1) \tag{23}$$

For these ζ_a and ζ_b values,

$$n = m.$$

Figures 8a and 8b show n and m as ordinates plotted against the abscissas ζ_a and ζ_b with ϑ as parameter. In itself (aside from the limiting cases) one of these two would suffice (ζ_a or ζ_b as abscissa). But for $\vartheta > 1$ the numerical calculation is more simple when ζ_a is used as variable, but for $\vartheta < 1$, ζ_b is preferable. Accordingly, the curves are more comprehensive when we select two different variables ζ_a and ζ_b for different ϑ. For $\vartheta = 1$, $\zeta_a = \zeta_b$ and the shape of the curves is the same (Compare equations 18 and 22).

Within the range of ζ_a and ζ_b considered here, and whose upper limit for $\vartheta > 1$ is given in equation (23), m is always imaginary (equation 22). For imaginary values of m and n we write, for short:

$$\left.\begin{aligned} \underline{m} &= \frac{m}{i} \\ \underline{n} &= \frac{n}{i} \end{aligned}\right\} \qquad (24)$$

For $\zeta_a = 0$ (and $\zeta_b = 0$) m has (independent of ϑ) the value $\underline{m} = \sqrt{3}$.

When ζ_a (ζ_b) increases, $\underline{m}$ increases at first (except for $\vartheta = \infty$). For $1 \leqq \vartheta \leqq \infty$, $\underline{m}$ becomes by

$$\zeta_a = \frac{4\vartheta}{\vartheta^2 - 1}$$

maximum

$$\underline{m}_{max} = \sqrt{\frac{3 + \frac{1}{\vartheta^2}}{1 - \frac{1}{\vartheta^2}}}$$

and then drops to a minimum:

$$\underline{m} = \sqrt{\frac{1 + \frac{1}{\vartheta}}{1 - \frac{1}{\vartheta}}},$$

which is reached by the limit value ζ_a in (23). For $0 \leqq \vartheta \leqq 1$, $\underline{m}$ tends uniformly to infinity. For $\zeta_a = 0$ ($\zeta_b = 0$) n is maximum

$$n_{max} = +1 \quad \text{(independent of } \vartheta\text{)}.$$

As $\zeta_a(\zeta_b)$ increases, n remains at first real and then drops evenly to a minimum $n = 0$, which with a perpendicular curve tangent is reached at

$$\left.\begin{aligned} \zeta_a &= \frac{1 + \sqrt{1 + 3\vartheta^2}}{\vartheta} \\ \text{and} \qquad \zeta_b &= \frac{1 + \sqrt{1 + 3\vartheta^2}}{\vartheta^2} \end{aligned}\right\} \tag{25}$$

When $\zeta_a(\zeta_b)$ exceeds this value, $\underline{n}$ becomes imaginary. For the highest ζ_a value considered here (equation 23) curve n with perpendicular tangent changes into curve $\underline{m}$. Likewise, of importance are functions

$$\left.\begin{aligned} &\text{a)} \quad \chi_a = \frac{n^2 - m^2}{\sqrt{\zeta_a}} \\ \text{and} \qquad &\text{b)} \quad \chi_b = \frac{n^2 - m^2}{\sqrt{\zeta_b}} \end{aligned}\right\} \tag{26}$$

illustrated in Figures (9a) and (9b). Both functions have an infinite value when $\zeta_a = 0$ and $\zeta_b = 0$. For $\vartheta > 1$, $/_a$ turns uniformly to zero, which it reaches with perpendicular tangent by

$$\zeta_a = \frac{2}{1 - \frac{1}{\vartheta}} \quad \text{(Compare equation 23).}$$

For $\vartheta < 1$, χ_b reaches a minimum

$$\chi_{b\,min} = 4\sqrt{1 + \sqrt{1 - \vartheta^2}}$$

at

$$\zeta_b = \frac{2}{\sqrt{1 - \vartheta^2}} \qquad (26')$$

Beginning at this minimum χ_b goes evenly to infinity when ζ_b increases. $\vartheta = 1$ yields a horizontal asymptote with ordinate 4. So, while χ_a and χ_b decrease when $\zeta_a(\zeta_b)$ increases beginning at $\zeta_a = 0$ and $(\zeta_b = 0)$, α and α^2 increase and approach infinity, so that the product $\alpha^2\ \chi_a$ (and $\alpha^2\ \chi_b$) (Compare equation 21) assumes a minimum value.

Every ϑ value and every $\zeta_a(\zeta_b)$ value within the range defined in (23) has a certain pair of n and m values (See equation 8) and, if beginning at $\zeta_a = 0$ $(\zeta_b = 0)$, n is at first real and m imaginary. This is why the letter i occurs in the numerator of φ and ψ in (20), and which is expressed by

$$\frac{\varphi}{i} = \frac{\sin 2\,n\,\alpha\ \underline{\sin}\ 2\,\underline{m}\,\alpha}{\cos 2\,n\,\alpha\ \underline{\cos}\ 2\,\underline{m}\,\alpha - \cos 4\,\alpha}$$

$$= \tan 2\,n\,\alpha\ \underline{\tan}\ 2\,\underline{m}\,\alpha\,\omega$$

The function φ/i* is shown plotted in Figure 10 for an arbitrarily chosen pair (according to equation 22) n (= 0.87) and

*The aim is to express that m as imaginary. If m and n are imaginary the expression φ/i^2 (instead of $-\varphi$) is used. ψ/i and ψ/i^2 are used in the same manner.

$\underline{m}$ (= 1.72) which corresponds to $\vartheta = 10$; $\zeta_a = 0.98$; the figure also includes $\tan 2\,n\,\alpha$ and ψ_f/i and ψ_e/i plotted against α (See equation 20). In a subsequent calculation of the critical shear stress we intend to show that n is never much lower than "one"; and even for materially lower n the course of function φ/i is not much different from that on Figure 10. The zero points of the function are usually at α values which form an integral multiple of $\pi/2n$, while the functions at those α values where the denominator disappears, have perpendicular asymptotes and change from $+\infty$ to $-\infty$. With $\alpha = 0$ denominator and numerator disappear; double differentiation of numerator and denominator of function φ yields

$$(\varphi)_{\alpha=o} = \frac{2\,n\,m}{4 - (n^2 + m^2)}$$

This, according to (20) is the value for ψ_e, so that

$$\left(\frac{\varphi}{i}\right)_{\alpha=o} = \frac{\psi_e}{i}$$

By $\alpha = 0$ function φ/i has a horizontal tangent as becomes evident for the reason that

$$\varphi(\alpha) = \varphi(-\alpha)$$

so that the function is symmetrical with respect to the ordinate axis. From $\alpha = 0$, φ goes evenly toward infinity. When $1 > n > 2/3$ there is an asymptote for a value α, which is somewhat higher than $\frac{1}{4}\,\frac{\pi}{n}$; in any case there is an asymptote near this value and another asymptote near $\frac{3}{4}\,\frac{\pi}{n}$, and between

the two φ intersects the axis of the abscissa when $\alpha = \frac{1}{2}\frac{\pi}{n}$.

Each φ/i function with a pair of n, m values has certain ψ_f/i and ψ_e/i values (equation 20) which are shown in Figures 12a and 12b plotted against ϑ and $\zeta_a(\zeta_b)$; ψ_f/i is always negative, and ψ_e/i positive. In Figure 10, ψ_f/i and ψ_e/i, being independent from α, are parallels of the axis of abscissa, and at $\alpha = 0$ the straight ψ_e/i is a tangent of function φ. The intersections of the straight ψ with curve φ yield α as solution of equation (20). For $\zeta_a = 0$ ($\zeta_b = 0$), ψ_f/i and ψ_e/i yield an absolute maximum, which is equivalent for every ϑ value.

For other possible pairs of n and m then in Figure 10, the same conditions prevail, when α is used as multiple of π/n; the position of the perpendicular asymptote and the ordinate of $(\varphi)_{\alpha=0}$ is slightly shifted. For n values near zero the straights ψ_f/i and ψ_e/i are very close to the axis of the abscissa, and coincide, like φ, with this axis when $n = 0$. Aside from this special case the solutions of equations $\varphi/i = \psi_f/i$ yield α values which are slightly lower than the integral multiple of $\pi/2n$, while $\varphi/i = \psi_e/i$ yields, aside from $\alpha = 0$, other α values which are slightly higher than the integral multiple of $\pi/2n$.

Being able to compute α by approximation, facilitates the solution. According to (20) $\varphi/1$ can be decomposed into

$$\frac{\varphi}{i} = \tan 2\,n\,\alpha \,\underline{\tan}\, 2\,\underline{m}\,\alpha\,\omega$$

$$\omega = \frac{1}{1 - \dfrac{\cos 4\,\alpha}{\cos 2\,n\,\alpha \,\underline{\cos}\, 2\,\underline{m}\,\alpha}}$$

$\underline{\tan}\ 2\ \underline{m}\ \alpha$ lies between 0 and 1; when $2\ \underline{m}\ \alpha$ increases it approaches "one" very quickly. Since $\underline{m}$ here is greater than n (in most cases twice as great as n), $\underline{\tan}\ 2\ \underline{m}\ \alpha$ is not much smaller than "one" for $\alpha \approx \pi/2\ n$ (for example, $\overset{\tan}{2}\ \pi = 0.999993$). The ω value for $\alpha = 1/8\ \pi$, $3/8\ \pi$, $5/8\ \pi$, etc. is "one" (unless $n = 1$), because then $\cos 4\alpha = 0$. By $\alpha = 1/4 \times \pi/n$, $3/4 \times \pi/n$, $5/4 \times \pi/n$, etc., $\omega = 0$, because $\cos 2\ n\ \alpha = 0$. For α values which satisfy equation $\cos 4\alpha = \cos 2\ n\alpha\ \underline{\cos}\ 2\ \underline{m}\ \alpha$, $\omega = \pm\infty$, because the denominator of ω disappears. On these points we find the asymptotes of curve φ/i. Figure 11 shows ω plotted against the φ/i curve of Figure 10. Near $\alpha = \pi/2\ n$, we approximate φ/i as

$$\frac{\varphi}{i} \approx \tan 2\ n\ \alpha .$$

Having defined an approximate value for α we compute $\omega\ \underline{\tan}\ 2\ \underline{m}\ \alpha$ and estimate the error of the approximation. The dotted line in Figure 10 represents the approximation curve $\tan 2\ n\ \alpha$.

Of all feasible solutions of equation $\varphi = \psi$, the solutions α near $\pi/2\ n$ represent only those values which yield the critical shear stress. Presuming this assertion correct, the functions $C_a = \alpha^2 \chi_a$ and $C_b = \alpha^2 \chi_b$ become minimum.

When $\vartheta > 1$, then α and α^2 are finite for $\zeta_a = 0$, and increase evenly when ζ_a increases; for n becomes smaller as ζ_a increases (Compare Figure 8a). Since the changes of ψ_f

and ψ_e in equation $\varphi/i = \psi/i$ (when ζ_a changes) have a relatively small effect on the α solutions, the α values are approximately inversely proportional to n and thus increase with ζ_a; when n goes to zero, α becomes infinite. But χ_a decreases evenly in this same range from $\chi_a = \infty$ (for $\zeta_a = 0$ and assumes for ζ_a, where $n = 0$ (See equation 25) a finite, real value. For $\zeta_a = 0$ and for ζ_a conformal to (25), the product of α^2 and χ_a becomes also infinite, while between it it assumes finite values.

For $\vartheta < 1$ the χ_b function becomes infinite at $\zeta_b = 0$ and $\zeta_b = \infty$; between these two is the minimum indicated by (26') α becomes finite for $\zeta_b = 0$. Aside from the limiting case $\vartheta = 0$, n decreases as ζ_b increases; when ζ_b approaches the value given by (25) - where $n = 0$ - then α becomes infinite. Between this value of ζ_b and $\zeta_b = 0$ the product of functions α^2 and χ_b has a minimum value.

That there is a minimum for $\alpha^2 \chi_b$ even if $\vartheta = 0$, was proved by Bergmann and Reissner.

When n is very small, α approaches infinity. When $n = 0$, any α satisfies equation $\varphi/i = \psi/i$.

When $\zeta_a(\zeta_b)$ increases beyond the value given in (25), for which $n = 0$, then n becomes imaginary. Since in this range $(n^2 + m^2)$ and χ_a and χ_b (26) decrease still further, it seems feasible that the minimum of $C_a(C_b)$ (equation 21) lies in just this range. With (24), equation (20) now becomes

$$\frac{\varphi}{i^2} = \frac{\psi_f}{i^2} \quad \text{and} \quad = \frac{\psi_e}{i^2}$$

$$\frac{\varphi}{i^2} = \omega \underline{\tan}\ 2\ \underline{n}\ \alpha \underline{\tan}\ 2\ \underline{m}\ \alpha$$

$$\omega = \frac{1}{1 - \dfrac{\cos 4\ \alpha}{\underline{\cos}\ 2\ \underline{n}\ \alpha \cos 2\ \underline{m}\ \alpha}}$$

$$\frac{\psi_f}{i^2} = -\frac{8\ \underline{n}\ \underline{m}}{4\ (\underline{n}^2 + \underline{m}^2) + (\underline{m}^2 - \underline{n}^2)^2}$$

$$\frac{\psi_e}{i^2} = \frac{2\ \underline{n}\ \underline{m}}{4 + (\underline{n}^2 + \underline{m}^2)}$$

Now ω and the product $\underline{\tan}\ 2\ \underline{n}\ \alpha \underline{\tan}\ 2\ \underline{m}\ \alpha$ are always positive, consequently φ/i^2 is positive also. But ψ_f/i^2 is always negative. In the case of free support this range of $\zeta_a(\zeta_b)$ yields no solution for α, except when $\underline{n} = 0$ $(n = 0)$. Otherwise a solution would be practicable only in the case of rigid restraint, because ψ_e/i^2 is always positive.

The shape of curve φ/i^2 with respect to α is like that of curve φ/i; Figure 13 shows φ/i^2 and $\underline{\tan}\ 2\ \underline{n}\ \alpha \underline{\tan}\ 2\ \underline{m}\ \alpha$ and ω plotted against α for $\underline{n} = 0.62$, $\underline{m} = 1.58$ (equivalent to $\vartheta = 5$, $\zeta_a = 2.2$), and for $\underline{n} = 1$; $\underline{m} = 1$ (equivalent to $\vartheta = \infty$, $\zeta_a = 2.0$), The straight line ψ_e/i^2 is again (as ψ_e/i by φ/i) the tangent to curve φ/i^2 at point $\alpha = 0$. While φ/i differs only slightly from $\tan 2\ n\ \alpha$ when α increases, the φ/i^2 function proceeds like the function $\underline{\tan}\ 2\ \underline{n}\ \alpha \underline{\tan}\ 2\ \underline{m}\ \alpha$ (in Figure 13), that is, approaches "one" asymptotically. The difference between φ/i^2 and function $\underline{\tan}\ 2\ \underline{n}\ \alpha \underline{\tan}\ 2\ \underline{m}\ \alpha$ is expressed in ω, which is also shown in Figure 13. When $\underline{n}$

becomes very small, φ/i^2 again (like φ/i) approaches the axis of the abscissa, and coincides with it when $\underline{n} = 0$ ($n = 0$). By the maximum value of ζ_a for $\underline{n}$ and $\underline{m}$ as given by (23), we obtain value "one" when $\vartheta = \infty$. All φ/i^2 curves for $\vartheta = \infty$ lie between this upper limit curve and the axis of abscissa. For smaller ϑ the limit curve (where $\underline{n} = \underline{m} \geq 1$) shifts upward, n and m become infinite when ϑ decreases and ζ_a increases. The limit curve φ/i^2 (where $\underline{n} = \underline{m}$) approaches when ϑ decreases toward "one," the straight line with the ordinate "one." It will be seen that in this range (for any $\underline{n}$ and $\underline{m}$) the only solution of the transcendent equation is the value $\alpha = 0$ for every ϑ value. For $\underline{n} = 0$ any value α fulfills the equation $\varphi/i^2 = \psi/i^2$ (like $\varphi/i = \psi/i$).

The next problem is to find which of the various solutions α yields the minimum $c_a = \alpha^2 \chi_a$ and $c_b = \alpha^2 \chi_b$ (equation 21). We begin with $\alpha = 0$ and case $n = 0$, where any α represents a solution of $\varphi = \psi$.

If $\alpha = 0$, we see from (13) that all four roots λ disappear, i.e., they are of the same magnitude ($\lambda_1 = \lambda_2 = \lambda_3 = \lambda_4$). In that case (11) does not yield the general integral for resolving the theorem in (11); instead of the four arbitrary constants we have only one. With four equal roots $\lambda_r = \lambda_1$ the solution (conformal to 11) of the differential equation reads:

$$w = e^{i\kappa \frac{x}{a}} e^{i\lambda_1 \frac{y}{a}} \left[C_1 + C_2 \left(\frac{y}{a}\right) + C_3 \left(\frac{y}{a}\right)^2 + C_4 \left(\frac{y}{a}\right)^3 \right]$$

The case of $n = 0$ is treated in the same manner; it yields $\lambda_1 = \lambda_2$, and in place of equation (11) for w we have

$$w = e^{i\kappa\frac{x}{a}}\left[e^{i\lambda_1\frac{y}{a}}\left(C_1 + C_2\frac{y}{a}\right) + e^{i\lambda_3\frac{y}{a}}C_3 + e^{i\lambda_4\frac{y}{a}}C_4\right]$$

Both cases $(\alpha = 0)$ and $(n = 0)$ yield a new theorem for function w, and equations (16) supply new equations whose determinant of the denominator, when made zero, leads to a relation between n, m, and α as expressed in theorem 1 (equation 11) by equations (17). The final result is that there is no function w - not zero - in the form called for by two or more equal roots λ_r. (Southwell and Skan made this examination for $\vartheta = 1$, and Bergmann and Reissner for $\vartheta = 0$, in Zeitschrift für Flugtechnik und Motorluftschiffahrt, Vol. 20, 1929, pp. 477-8.)

This leaves us the solutions α which are near the integral multiples of $\pi/2n$ and which result from an equation $\varphi/i = \Psi/i$ (where n is real).

Since we seek the minimum value of shear t, that is, of C_a and C_b (See equation 21), the solution α near $\pi/2n$ is the only one to be considered for every ϑ value. For the case (f) of free support α is slightly lower; for (e) rigid restraint somewhat higher than $\pi/2n$.

Now we can develop a formula for c_a and c_b (equation 21'). Within the range considered

$$\alpha = \frac{1}{2n}\arctan\frac{\Psi}{\omega}$$

can be very accurately approximated by introducing for ω a corresponding approximative function or simply a constant ($\omega \approx 1$).

Writing the approximated α in (21) it is probable that a differentiation yields an analytical function for the minimum $C_a(C_b)$ with variable ϑ. But this function which the equation would (approximately) represent (See Figures 2a and 2b) would be very complicated and unsuited to practical use. For that reason we preferred to calculate a series of points on this curve and to express the result graphically in Figures 2a and 2b.

9. Calculation of c_a and c_b for various ϑ values.- For $\vartheta > 1$ we have a range of ζ_a limited by $\zeta_a = 0$ and ζ_a as defined in equation (25). For $\vartheta < 1$ the range is between $\zeta_b = 0$ and ζ_b as defined in (26'). For any ζ_a and ζ_b values within this range, we have

$\frac{n^2 + m^2}{2}$, $\frac{n^2 - m^2}{2}$, n, m and n m (according to eq. 22)

χ (" " " 26)

ψ and α (" " " 20)

C_a " C_b (" " " 21)

The sign of n and m is, according to (22), either positive or negative, but we confine ourselves to the positive, because the negative sign yields the same result. For, changing the sign by m($\underline{m}$) or n that for $\varphi(\varphi/i)$ and $\psi(\psi/i)$ changes also, so that (20), (21) and (26) are not altered. The sign for α, which likewise can be positive or negative (Compare (20))

has no effect on the final result, because it is affected only by the direction of t (Compare (14c), which may be arbitrarily assumed.

The solution of (20) is approximated with $\omega = 1$ [that is, $\alpha = (\frac{1}{2} n) \arctan \psi$], the solution α being inserted only near $\pi/2n$. This is a very satisfactory approximation for the case of rigid restraint.

By $\zeta_a = 0$ ($\zeta_b = 0$) we find $n = 1$ and $\underline{m} = \sqrt{3}$ for all ϑ values; and as α minimum we find:

$\alpha = 1.306$ (approximated = 1.309) by free support.

$\alpha = 1.8330$ (" = 1.8333) by rigid restraint.

As example, Figure 14 shows the functions $\frac{1}{2}\chi_a$, α, $\underline{n}$, m/i, and $1/10$ C_a plotted against ζ_a for $\vartheta = 5$ by free edge support. The range of ζ_a has been enlarged beyond practical use. For $\vartheta = 1$ the minimum c_a (c_b) of C_a (C_b) is at $\zeta_a > 0.7$ ($\zeta_b > 0.7$), for $\vartheta = 0$ at $\zeta_b < 1.35$ and for $\vartheta = \infty$ at $\zeta_a \approx 1.0$.

The range of ζ_a and ζ_b for practical purposes is:

ζ_a = 0.7 to 1.0 for $\vartheta > 1$, free support

ζ_b = 0.7 " 1.35 " $\vartheta < 1$, " "

ζ_a = 0.9 " 1.1 " $\vartheta > 1$, rigid restraint

ζ_b = 0.9 " 2.25 " $\vartheta < 1$, " "

For $\vartheta = 0$, 1/5, 1/2, 1 and $\vartheta = 2$, 3, 5, 10, 20, 40 and ∞, the calculations are shown in Table I and tabulated in Table II.

The figures for c_a (for $\vartheta \geqq 1$) and c_b (for $\vartheta \leqq 1$)

were rounded off to five units, the calculation was made with corresponding accuracy (i.e., the error for c_a and c_b does not exceed 0.3 per cent). In Figures 2a and 2b, c_a and c_b are plotted against ϑ.

10. Equation and calculation of c_a' and c_b' derived for the wave length of the elastic surface.- Equation (11) expresses the elastic surface of the strip when wrinkling under shear. It contains, aside from a, the five constants κ, C_1, C_2, C_3, and C_4, of which the four constants can be computed from the linear homogeneous equations (16). The κ constant defines the wave length of the elastic surface in the x-direction. According to (18) we have

$$\kappa = \alpha \sqrt{\zeta_a} \sqrt[4]{\frac{D_2}{D_1}} = \frac{\alpha \sqrt{\zeta_a}}{\sqrt[4]{\rho}} \quad \text{and} \quad = \alpha \sqrt{\zeta_b} \sqrt{\frac{D_2}{D_3}} = \frac{\alpha \sqrt{\zeta_b}}{\sqrt{\mu}}$$

There are five constants for every pair of ϑ, ζ_a and ϑ, ζ_b or, in other words, every pair has a corresponding elastic surface, which in a homogeneous orthogonal-anisotropic plate would become that of the shear t_{kr}. But since the usual stiffened plate never exactly agrees with our assumed ideal system, the elastic surface of a plate when wrinkling deviates more or less from the calculation here.

Since

$$e^{i\kappa\frac{x}{a}} = \cos\left(\kappa \frac{x}{a}\right) + i \sin\left(\kappa \frac{x}{a}\right)$$

we infer from equation (11) that the half-wave l of the elastic surface equals half the period of the sine function, that is,

$$l = \frac{\pi}{\kappa} a.$$

So, when we introduce κ conformal to (18) the wave length is computed as

$$\left.\begin{aligned} &a) \quad l = C_a' \, a \sqrt[4]{\frac{D_1}{D_2}} \qquad \frac{l}{a} = C_a' \sqrt[4]{\rho} \\ &b) \quad l = C_b' \, a \sqrt{\frac{D_3}{D_2}} \qquad \frac{l}{a} = C_b' \sqrt{\mu} \end{aligned}\right\} \tag{27}$$

where

$$C_a' = \frac{\pi}{\alpha \sqrt{\zeta_a}}; \qquad C_b' = \frac{\pi}{\alpha \sqrt{\zeta_b}} = C_a' \sqrt{\vartheta} \quad \text{(Compare eq. 18b)}$$

If the respective shear equals the shear strength t_{kr}, we substitute l_{kr} and c_a' and c_b' for l, C_a' and C_b', so that (4a) and (4b) yield

$$\begin{aligned} l_{kr} &= c_a' \, a \sqrt[4]{\frac{D_1}{D_2}} \qquad \frac{l_{kr}}{a} = c_a' \sqrt[4]{\rho} \\ l_{kr} &= c_b' \, a \sqrt{\frac{D_3}{D_2}} \qquad \frac{l_{kr}}{a} = c_b' \sqrt{\mu} \end{aligned}$$

The calculation of C_a' and C_b' made by equation (27) for various ϑ, ζ_a and ζ_b is shown in Table I (columns 9 and 13). The values for c_a' and c_b' are accurately computed to 1 to 3 per cent.

Figure 15a shows $C_a = t \, a^2 / \sqrt[4]{D_1 \, D_2^3}$ plotted against $C_a' = \frac{l}{a} \frac{1}{\sqrt[4]{\rho}}$. When l (C_a') changes near the minimum (c_a) of C_a, the change in t (C_a) is comparatively slight, particularly by free support.

Figure 15b exhibits $C_b = t \, a^2 / \sqrt{D_2 \, D_3}$ plotted against $C_b' = \frac{l}{a} \frac{1}{\sqrt{\mu}}$. This figure likewise shows the slight change in t (C_b') when l (C_b') changes near the minimum c_b) of C_b.

References

1. Southwell, R. V. and Skan, Sylvia W. : On the Stability Under Shearing Forces of a Flat Elastic Strip. Proceedings of the Royal Society, 1924, Series A, Vol. 105, No. A 733.

2. Bergmann, St. and Reissner, H. : Buckling of Corrugated Strips Subjected to Shear Stresses. Zeitschrift für Flugtechnik und Motorluftschiffahrt, 1929, p. 475; and Z.F.M., 1930, p. 306.

3. Schmieden, C. : Buckling of Stiffened Plates in Shear. Zeitschrift für Flugtechnik und Motorluftschiffahrt, Vol. 21, 1930, p. 61

4. Huber, M. T. (Lemberg) : The Theory of Crosswise Reinforced Concrete Steel Plates with Applications to Various Structurally Important Problems on Rectangular Plates. Bau-Ingenieur, 1923, Nos. 12-13, p. 354.

Translation by J. Vanier,
National Advisory Committee
for Aeronautics.

TABLE I

Calculation of coefficients C_a (C_b) and $C_{a'}$ ($C_{b'}$). The figures for the shear strength t_{kr}, i.e. for minimum C_a and C_b are underscored.

1	2	3	4	5	6	7	8	9	10	11	12	13
					Free Support				Rigid Restraint			
ϑ	ξ_b	n	$\underline{m} = \frac{m}{i}$	χ_b	$-\frac{\psi_f}{i}$	α	C_b	$C_{b'}$	$\frac{\psi_e}{i}$	α	C_b	$C_{b'}$
According to equation		22	22	26	20	20	21	27	20	20	21	27
	0.3		1.898	8.400	0.4803	1.3469	15.24	4.265	0.576	1.8325	28.20	3.13
	0.5		2.000	7.075	0.4320	1.3670	13.220	3.255	0.5715	1.8304	23.72	2.43
	1.0		2.236	6.000	0.3440	1.4047	11.839	2.238	0.559	1.8256	20.04	1.72
	1.30		2.3664	5.7886	0.3055	1.4222	11.7085	1.9374				
	1.32		2.3749	5.7794	0.3033	1.4233	11.7079	1.9212				
	1.34		2.3833	5.7796	0.3010	1.4244	11.7081	1.9053				
	2.00		2.64575	5.6568*)	0.2405	1.4528	11.939	1.529	0.5292	1.8144	18.6227	1.224
	2.22		2.7276	5.6646					0.5225	1.8116	18.5894	1.1639
0	2.24	1	2.7350	5.6659					0.5219	1.8113	18.5889	1.1588
	2.26		2.7423	5.6674					0.5213	1.8111	18.5896	1.1539
	2.5		2.827	5.690	0.2078	1.4684	12.260	1.353	0.5142	1.8083	18.62	1.10
	3.0		3.000	5.775					0.500	1.8025	18.75	1.01
	4.0		3.315	6.000	0.1443	1.4990	13.450	1.047	0.474	1.7921	19.27	0.88
	8.0		4.359	7.071	0.0739	1.5340	16.640	0.724	0.396	1.760	21.89	0.63
	20.0		6.554	9.850	0.0249	1.5583	23.88	0.452	0.285	1.7100	28.83	0.41
	30.0		7.933	11.690	0.0143	1.5636	28.60	0.367	0.240	1.6885	33.28	0.34
	50.0		10.149	14.708	0.0072	1.566	36.070	0.284				

* $\chi_{b\ min}$

TABLE I (cont.)

1	2	3	4	5	6	7	8	9	10	11	12	13
					Free Support				Rigid Restraint			
ϑ	ξ_b	n	$m = \frac{m}{i}$	χ_b	$-\frac{\psi_f}{i}$	α	C_b	C_b'	$\frac{\psi_e}{i}$	α	C_b	C_b'
According to equation		22	22	26	20	20	21	27	20	20	21	27
	1.24	0.995	2.339	5.8022	0.3121	1.4260	11.798	1.978				
	1.27	0.995	2.352	5.7857	0.3086	1.4279	11.797	1.953				
	1.28	0.995	2.356	5.7806	0.3074	1.4285	11.796	1.944				
	1.30	0.995	2.365	5.7707	0.3051	1.4298	11.797	1.927	0.546	1.833	19.40	1.506
1/5	2.00	0.9899	2.642	5.6285	0.2395	1.4681	12.13	1.513	0.523	1.8302	18.8527	1.214
	2.04	0.9896	2.657	5.6282*)					0.522	1.8302	18.8523	1.202
	2.05	0.9895	2.6607	5.6282					0.521	1.8302	18.8526	1.199
	2.08	0.9893	2.6718	5.6285					0.520	1.8303	18.8538	1.195
	0.4	0.995	1.947	7.564	0.4564	1.363	14.05	3.65	0.573	1.840	25.64	2.702
	1.08	0.9758	2.2610	5.836	0.3304	1.4459	12.199	2.091				
	1.10	0.9755	2.2697	5.819	0.3277	1.4476	12.195	2.069	0.541	1.864	20.22	1.605
	1.12	0.9743	2.2780	5.800	0.3249	1.4506	12.206	2.144				
	1.40	0.9629	2.3932	5.624					0.5237	1.8818	19.915	1.411
1/2	1.50	0.9525	2.4329	5.583					0.5182	1.8881	19.903	1.359
	1.60	0.9538	2.4718	5.550					0.5125	1.8951	19.931	1.311
	2.00	0.936	2.62	5.475	0.2335	1.556	13.24	1.427	0.4904	1.921	20.15	1.156
	2.309			5.464*)								
	4.00	0.8105	3.2645	5.653	0.1260	1.860	19.567	0.845	0.408	2.013	22.85	0.780
	6.00	0.6451	3.7942	6.055	0.0710	2.3800	34.298	0.538	0.269	2.658	42.85	0.482
	8.00	0.4064	4.2621	6.477	0.0340	3.824	94.8	0.448				

* $\chi_{b\ min}$

TABLE I (cont.)

1	2	3	4	5	6	7	8	9	10	11	12	13
					Free Support				Rigid Restraint			
ϑ	ξ_b	n	$\underline{m} = \frac{m}{i}$	χ_b	$-\frac{\psi_f}{i}$	α	C_b	$C_{b'}$	$\frac{\psi_e}{i}$	α	C_b	$C_{b'}$
According to equation		22	22	26	20	20	21	27	20	20	21	27
	0.182	0.9962	1.8321	10.194					0.5736	1.8382	34.444	4.006
	0.3306	0.9883	1.907			1.366	14.97	4.00				
	0.4025	0.9828	1.9419							1.858	25.78	2.665
	0.6813	0.9548	2.0673							1.903	22.75	2.000
	0.70	0.9527	2.0755	6.2336	0.3877	1.4538	13.1739	2.5829				
	0.73	0.9490	2.0882	6.1578	0.3818	1.4622	13.1649	2.5147				
	0.74	0.9477	2.0924	6.1337	0.3799	1.4650	13.1647	2.4928				
	0.75	0.9464	2.0966	6.1101	0.3780	1.4679	13.1656	2.4713				
	0.80	0.9398	2.1174	6.0000	0.3685	1.4826	13.1893	2.3690				
	0.90	0.9256	2.1580	5.8119					0.5122	1.9527	22.1600	1.6959
	0.92	0.9227	2.1659	5.7785					0.5098	1.9580	22.1528	1.6728
1**)	0.93	0.9211	2.1699	5.7623					0.5086	1.9607	22.1513	1.6615
	0.94	0.9196	2.1739	5.7464					0.5074	1.9634	22.1520	1.6504
	0.96	0.9165	2.1817	5.7155					0.5049	1.9690	22.1577	1.6285
	1.0191	0.9062	2.2044			1.556	13.63	2.000				
	1.2811	0.8595	2.3040							2.079	23.07	1.335
	1.5442	0.8021	2.3967							2.208	25.00	1.145
	1.6181	0.7849	2.4211			1.850	17.42	1.335				
	1.778	0.7453	2.4721							2.355	27.718	1.001
	2.0299	0.6707	2.5515			2.205	23.77	1.000				
	2.1248	0.6411	2.5809							2.694	35.22	0.800
	2.5370	0.5023	2.6832			2.996	42.56	0.665				
	2.6773	0.3958	2.7404			3.840	69.20	0.500				

**For $\vartheta = 1$ we used in part Southwell & Skan's data.

TABLE I (cont.)

1	2	3	4	5	6	7	8	9	10	11	12	13
					Free Support				Rigid Restraint			
ϑ	ζ_a	n	$\underline{m} = \frac{m}{i}$	χ_a	$-\frac{\psi_f}{i}$	α	C_a	$C_{a'}$	$\frac{\psi_e}{i}$	α	C_a	$C_{a'}$
According to equation		22	22	26	20	20	21	27	20	20	21	27
	0.30	0.988	1.810	7.77	0.524	1.346	14.08	4.265	0.568	1.851	26.62	3.096
	0.70	0.9451	1.8956	5.365	0.4634	1.4307	10.975	2.624	0.5358	1.921	19.77	1.956
	0.80	0.9288	1.9138	5.0596	0.4489	1.4626	10.823	2.402	0.5228	1.9504	19.247	1.801
	0.86	0.9180	1.9242	4.9014	0.4402	1.4839	10.793	2.283				
	0.90	0.9103	1.9310	4.8039	0.4344	1.4992	10.797	2.209	0.5095	1.9843	18.915	1.669
2	0.95	0.9002	1.9392	4.6930	0.4272	1.5195	10.828	2.126	0.5024	2.0035	18.824	1.608
	0.99	0.8917	1.9455	4.6034	0.4213	1.5369	10.8741	2.054	0.4964	2.0199	18.783	1.563
	1.01	0.8874	1.9487	4.5620	0.4185	1.5458	10.9012	2.022	0.4934	2.0284	18.770	1.540
	1.03	0.8828	1.9518	4.5214					0.4902	2.0375	18.771	1.519
	1.50	0.7458	2.015	3.7660	0.3406	1.886	13.390	1.361	0.4010	2.362	20.99	1.084
	1.66	0.6795	2.032	3.5560	0.3097	2.8404	15.535	1.166	0.3603	2.568	23.45	0.947
	2.00	0.4845	2.056	3.1600	0.2201	3.020	28.89	0.735	0.249	3.496	38.70	0.635
	0.87	0.9101	1.8462	4.5421	0.4755	1.4802	9.9548	2.2755				
	0.90	0.9037	1.8484	4.4622	0.4718	1.4925	9.9404	2.2187	0.5062	2.0026	17.895	1.6536
	0.93	0.8970	1.8505	4.3853	0.4681	1.5055	9.9393	2.1639				
	0.96	0.8899	1.8526	4.3114	0.4644	1.5190	9.9484	2.1120				
3	0.99	0.8827	1.8545	4.2397					0.4916	2.0383	17.6141	1.5491
	1.05	0.8674	1.8581	4.1034	0.4520	1.5680	10.07	1.955	0.4811	2.0694	17.5716	1.4816
	1.11	0.8509	1.8612	3.9751					0.4699	2.1041	17.5991	1.4172
	1.20	0.8237	1.8651	3.7948	0.4317	1.660	10.46	1.810	0.4518	2.1645	17.7792	1.3249

TABLE I (cont.)

1	2	3	4	5	6	7	8	9	10	11	12	13
					Free support				Rigid restraint			
ϑ	ζ_a	n	$\underline{m} = \frac{m}{i}$	χ_a	$-\frac{\psi_f}{i}$	α	C_a	C_a'	$\frac{\psi_e}{i}$	α	C_a	C_a'
According to equation		22	22	26	20	20	21	27	20	20	21	27
	0.20	0.995	1.752	9.079	0.5623	1.321	15.849	5.317	0.5735	1.840	30.747	3.818
	0.30	0.989	1.760	7.442	0.5552	1.332	13.305	4.306	0.5689	1.850	25.465	3.101
	0.40	0.980	1.766	6.46	0.5475	1.351	11.80	3.679	0.5623	1.8635	22.415	2.666
	0.50	0.970	1.732	5.78	0.54	1.365	10.744	3.255	0.5541	1.8815	20.421	2.361
	0.75	0.93	1.779	5.38					0.5244	1.9487	17.69	1.863
	0.92	0.8926	1.7790	4.1302	0.5048	1.4958	9.2426	2.1900				
	0.95	0.8850	1.7785	4.0490	0.5018	1.5100	9.2290	2.1338				
5	0.98	0.8770	1.7780	3.9703	0.4987	1.5256	9.2403	2.0801				
	1.00	0.8716	1.7775	3.9192	0.4965	1.5383	9.2743	1.9596	0.4841	2.0609	16.647	1.525
	1.075	0.8495	1.7753	3.7340					0.4691	2.1071	16.586	1.438
	1.15	0.8246	1.7720	3.5621					0.4523	2.1623	16.655	1.355
	1.25	0.787	1.766	3.347	0.4635	1.726	9.965	1.628	0.4277	2.2527	16.98	1.248
	1.50	0.666	1.745	2.850	0.412	2.066	12.155	1.238	0.3521	2.6127	19.43	0.982
	1.75	0.467	1.708	2.371	0.3094	3.0404	21.919	0.781	0.2383	3.6116	30.93	0.658
	1.80	0.408	1.699	2.275	0.2744	3.5235	28.248	0.665	0.2062	4.1011	38.27	0.571
	1.85	0.336	1.690	2.180	0.2300	4.335	41.00	0.533	0.1687	4.925	52.9	0.469
	0.96	0.8759	1.7203	3.8032	0.5321	1.5113	8.6865	2.1216				
	0.97	0.8730	1.7194	3.7755	0.5312	1.5168	8.6861	2.1030				
	0.98	0.8701	1.7184	3.7477	0.5305	1.5222	8.6836	2.0848				
	0.99	0.8671	1.7175	3.7204	0.5296	1.5279	8.6854	2.0665				
10	1.00	0.8641	1.7166	3.6932	0.5288	1.5336	8.6859	2.0485				
	1.07	0.8415	1.7094	3.5094					0.4630	2.1244	15.8375	1.4297
	1.08	0.8381	1.7083	3.4839					0.4606	2.1319	15.8347	1.4180
	1.09	0.8346	1.7072	3.4587					0.4583	2.1396	15.8340	1.4064
	1.10	0.8310	1.7060	3.4336					0.4559	2.1476	15.8358	1.3948
	1.11	0.8274	1.7049	3.4086					0.4534	2.1557	15.8400	1.3832

TABLE I (cont.)

1	2	3	4	5	6	7	8	9	10	11	12	13
					Free Support				Rigid Restraint			
ϑ	ζ_a	n	$m = \frac{m}{i}$	χ_a	$-\frac{\psi_f}{i}$	α	C_a	$C_{a'}$	$\frac{\psi_e}{i}$	α	C_a	$C_{a'}$
According to equation		22	22	26	20	20	21	27	20	20	21	27
	0.80	0.914	1.708	4.1949	0.5570	1.438	8.66	2.44				
	0.95	0.876	1.682	3.7223	0.5472	1.504	8.43	2.15				
	1.00	0.860	1.665	3.5792	0.5470	1.533	8.42	2.05	0.4751	2.084	15.549	1.507
	1.05	0.843	1.679	3.4430	0.5426	1.566	8.44	1.96				
20	1.08	0.8325	1.674	3.3628					0.4562	2.144	15.458	1.410
	1.10	0.825	1.671	3.3098					0.4513	2.160	15.448	1.386
	1.12	0.817	1.667	3.2590					0.4460	2.178	15.463	1.363
	1.15	0.805	1.662	3.1828					0.4378	2.207	15.499	1.328
	1.20	0.785	1.653	3.0600	0.5270	1.690	8.71	1.693	0.4234	2.260	15.618	1.299
	0.98	0.8643	1.6721	3.5790	0.5572	1.5199	8.2678	2.0879				
	1.00	0.8578	1.6691	3.5217	0.5560	1.5320	8.2655	2.0507				
	1.02	0.8511	1.6660	3.4653	0.5546	1.5447	8.2682	2.0138				
40	1.05	0.8407	1.6611	3.3824					0.4614	2.1256	15.2823	1.4424
	1.08	0.8297	1.6560	3.3011					0.4539	2.1501	15.2606	1.4060
	1.10	0.8220	1.6525	3.2478					0.4487	2.1675	15.2584	1.3820
	1.12	0.8141	1.6488	3.1951					0.4433	2.1854	15.2597	1.3584
	1.15	0.8016	1.6432	3.1170					0.4349	2.2154	15.2984	1.3224

TABLE I (cont.)

1	2	3	4	5	6	7	8	9	10	11	12	13
					Free Support				Rigid Restraint			
ϑ	ζ_a	n	$m = \frac{m}{i}$	χ_a	$-\frac{\psi_f}{i}$	α	C_a	$C_{a'}$	$\frac{\psi_e}{i}$	α	C_a	$C_{a'}$
According to equation		22	22	26	20	20	21	27	20	20	21	27
	0.15	0.996	1.730	10.2918	0.577	1.320	17.96	6.15	0.5743	1.839	34.82	4.4075
	0.25	0.992	1.727	9.9720	0.577	1.319	13.6	4.7625	0.5707	1.843	27.00	3.405
	0.50	0.9675	1.714	5.4758	0.577	1.353	10.00	3.295	0.56	1.887	19.52	2.36
	0.75	0.924	1.689	4.2816	0.574	1.421	8.63	2.570	0.52	1.96	16.44	1.853
	0.95	0.872	1.661	3.6114	0.5684	1.509	8.139	2.147				
	0.98	0.8623	1.6563	3.5224	0.5667	1.519	8.128	2.0896				
	1.00	0.8556	1.6527	3.464	0.5656	1.5315	8.125	2.0515	0.4714	2.092	15.14	1.5025
	1.02	0.8487	1.6493	3.4069	0.5644	1.5445	8.127	2.014				
	1.05	0.8379	1.6438	3.3222	0.5625	1.5655	8.142	1.958	0.4591	2.1312	15.089	1.4385
∞	1.08	0.8266	1.6381	3.2395					0.4514	2.1566	15.067	1.4017
	1.10	0.8185	1.6340	3.1846					0.4458	2.1750	15.065	1.377
	1.12	0.8105	1.630	3.1312					0.4403	2.1936	15.067	1.3535
	1.15	0.7975	1.624	3.0517					0.4317	2.225	15.108	1.3165
	1.25	0.749	1.600	2.7924	0.540	1.768	8.74	1.573	0.3993	2.352	15.43	1.195
	1.40	0.654	1.560	2.4138	0.505	2.045	10.10	1.299	0.3397	2.652	16.95	1.000
	1.50	0.568	1.524	2.1604	0.462	2.388	12.33	1.073	0.2887	3.015	19.68	0.85
	1.60	0.447	1.483	1.8974	0.3866	3.100	18.23	0.801	0.2213	3.76	26.73	0.66
	1.65	0.359	1.468	1.7579	0.3218	3.945	27.3	0.62	0.1758	4.62	37.35	0.53
	1.66	0.342	1.453	1.7339	0.3062	4.16	29.95	0.586				
	1.70	0.333	1.433	1.6168	0.214	6.32	64.65	0.382				

TABLE II

Recapitulation of shear strength factors: c_a and c_b (for computing t_{kr} according to 1a and 1b) and c_a' and c_b' (for computing the conformal wave length l_{kr} of the elastic surface according to 4a and 4b).

1	2	3	4	5	6	7	8	9
ϑ	Free support				Rigid restraint			
	c_a	c_b	c_a'	c_b'	c_a	c_b	c_a'	c_b'
0	∞	11.71	∞	1.92	∞	18.59	∞	1.16
1/5	26.4	11.8	4.35	1.94	42.15	18.85	2.69	1.20
1/2	17.25	12.2	2.93	2.07	28.15	19.9	1.92	1.36
1	13.165	13.165	2.49	2.49	22.15	22.15	1.66	1.66
2	10.8	15.25	2.28	3.23	18.75	26.55	1.54	2.18
3	9.95	17.2	2.16	3.75	17.55	30.45	1.48	2.57
5	9.25	20.65	2.13	4.77	16.6	37.1	1.44	3.22
10	8.7	27.45	2.08	6.59	15.85	50.05	1.41	4.45
20	8.4	37.65	2.05	9.17	15.45	69.1	1.39	6.20
40	8.25	52.25	2.05	12.97	15.25	96.5	1.38	8.74
∞	8.125	∞	2.05	∞	15.065	∞	1.38	∞

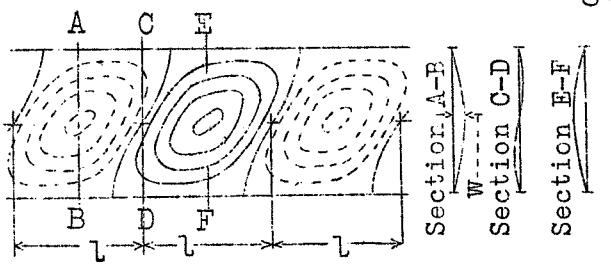

Fig.1 Elastic surface (contours and sections) of orthogonal anisotropic plate strip when wrinkling. Deflection w varies periodically in the longitudinal direction of the strip. The distance of the ensuing junction lines (the half-wave length) is l.

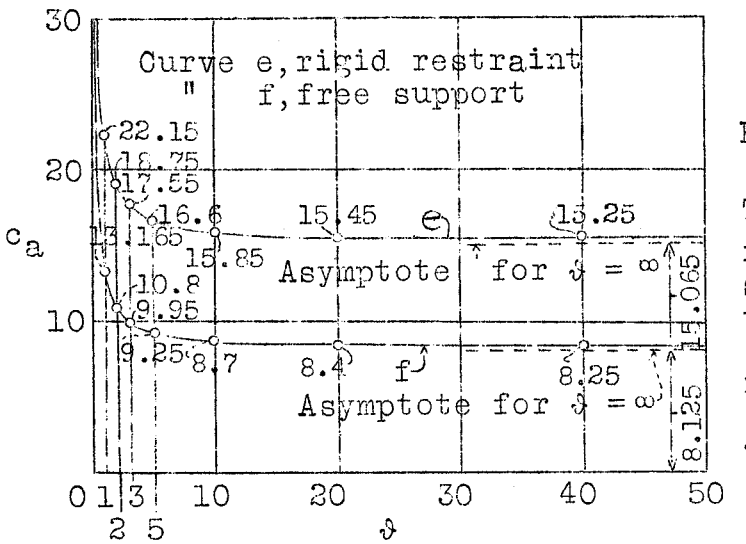

Fig.2a c_a plotted against ϑ. The coefficient c_a in the equation of shear strength $t_{kr}=c_a\sqrt{D_1D_2^3/a^2}$ is dependent on $\vartheta=\sqrt{D_1D_2/D_3}$

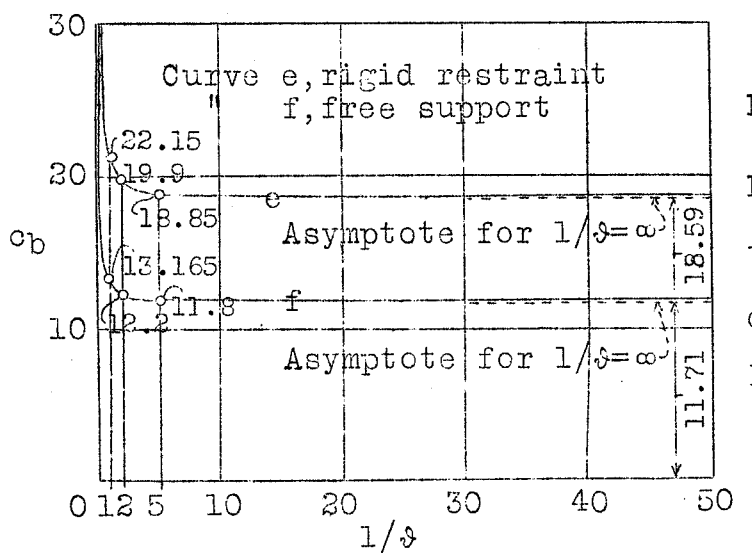

Fig.2b c_b plotted against $1/\vartheta$. Factor c_b in formula $t_{kr}=c_b\sqrt{D_2D_3/a^2}$ is dependent on $1/\vartheta=D_3/\sqrt{D_1D_2}$

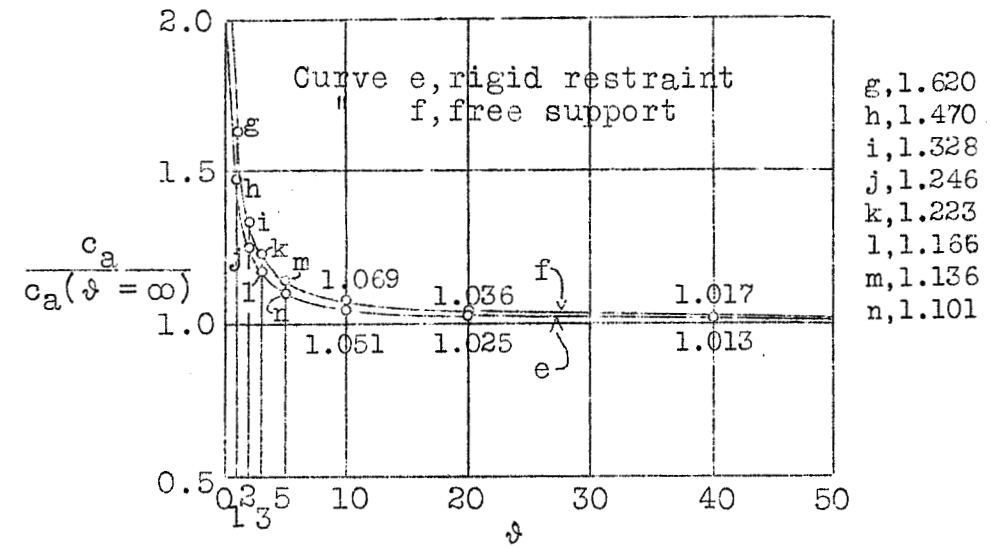

Fig.3a Quotient $c_a/c_a(\vartheta = \infty)$ plotted against ϑ.

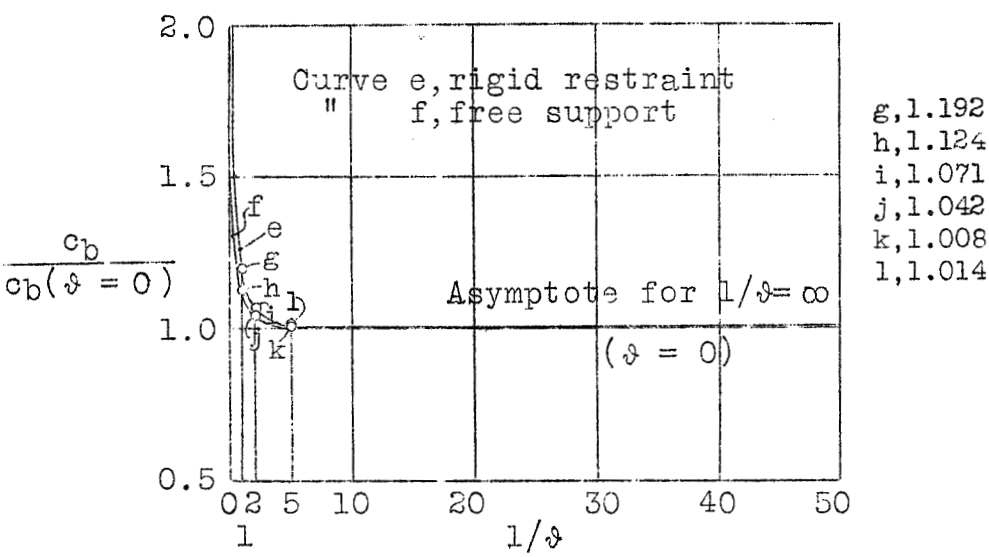

Fig.3b Quotient $c_b/c_b(\vartheta = 0)$ plotted against $1/\vartheta$.

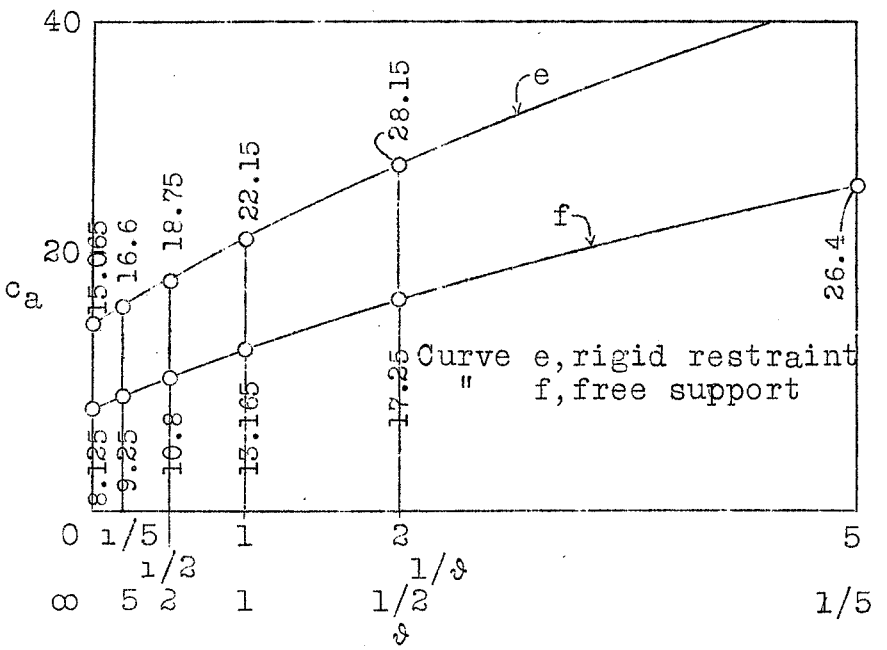

Fig.4a c_a plotted against $1/\vartheta$

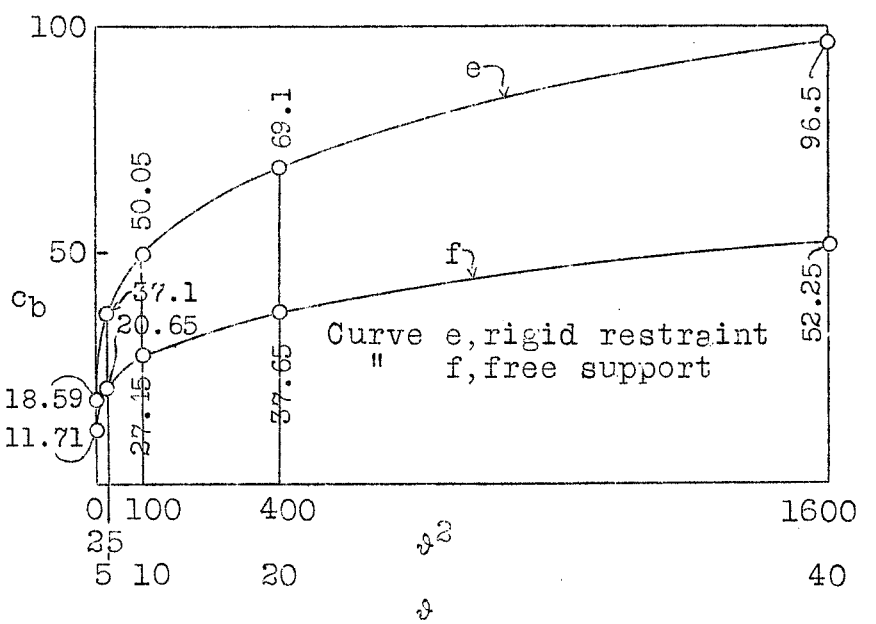

Fig.4b c_b plotted against ϑ^2

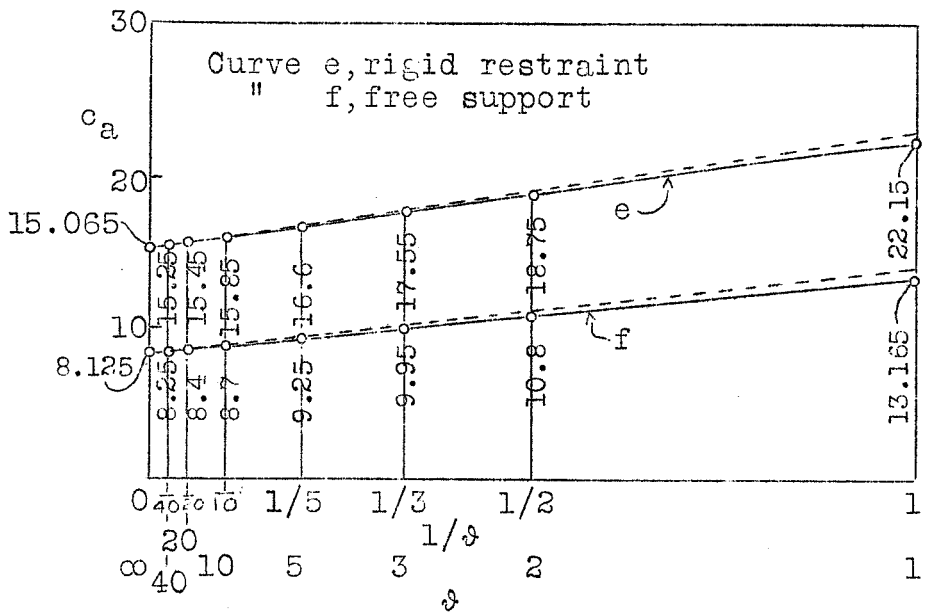

Fig.5a c_a plotted against $1/\vartheta$ within range of $0 \leqq 1/\vartheta \leqq 1$

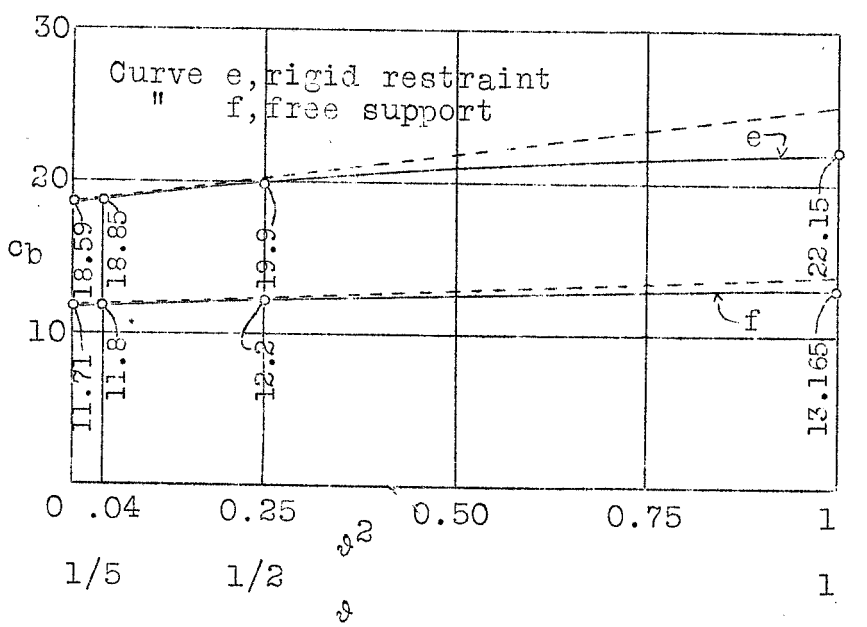

Fig.5b c_b plotted against ϑ^2 within range of $0 \leqq \vartheta^2 \leqq 1$

Curve e, rigid restraint
" f, free support

m,1.44
n,2.13
g,2.49
h,1.66
i,2.28
j,1.54
k,1.48
l,2.16

Fig.6a c_a' plotted against ϑ.

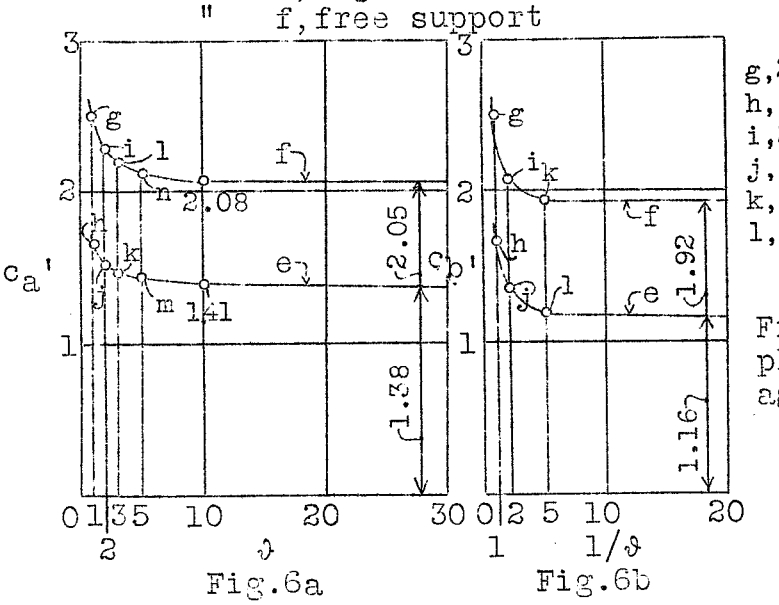

Fig.6a

Fig.6b

g,2.49
h,1.66
i,2.07
j,1.36
k,1.94
l,1.20

Fig.6b c_b' plotted against $1/\vartheta$

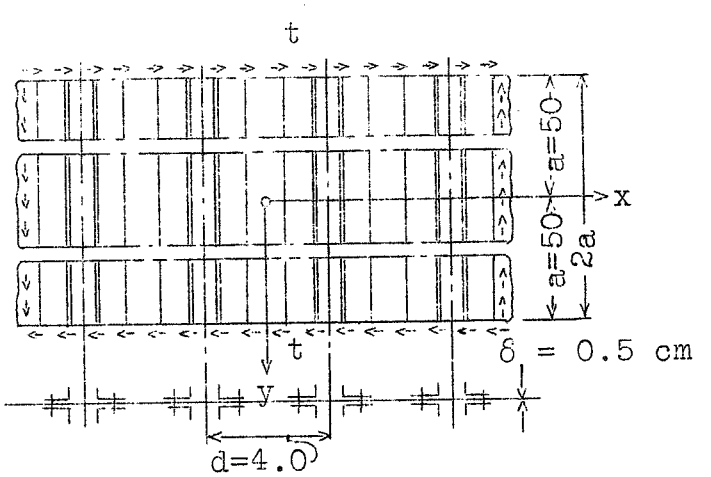

Fig.7 Section of reinforced plate (example).

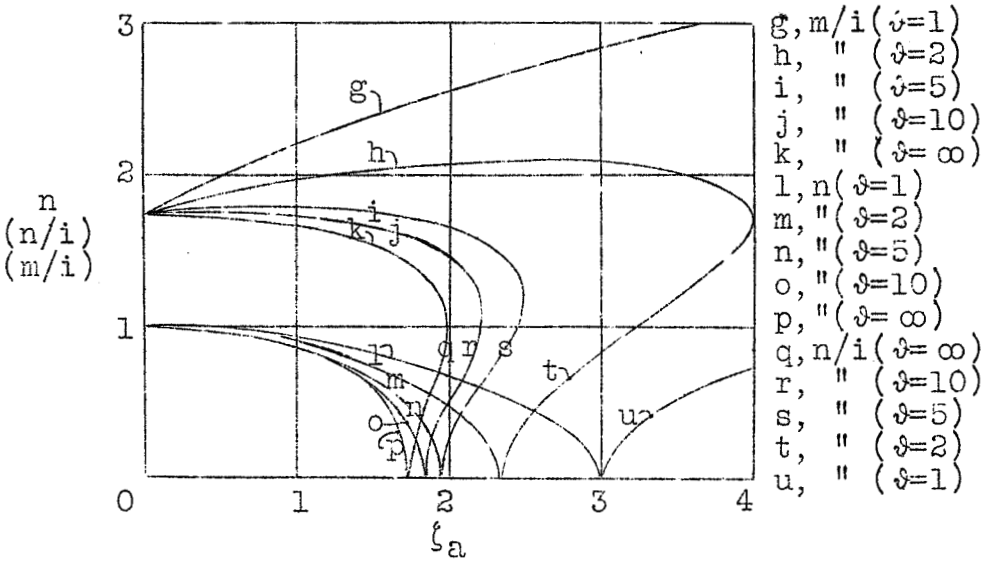

Fig.8a n(n/i=n) and m/i(=m) plotted against ζ_a and ϑ ($1 \leqq \vartheta \leqq \infty$).(Compare equation 22)

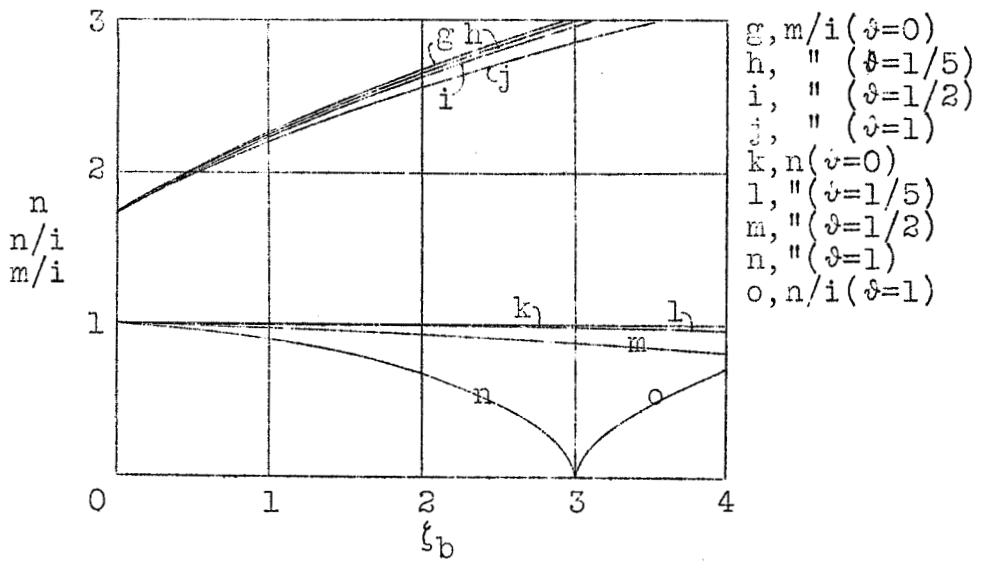

Fig.8b n(n/i=n) and m/i(=m) plotted against ζ_b and ϑ ($0 \leqq \vartheta \leqq 1$)(see equation 22)

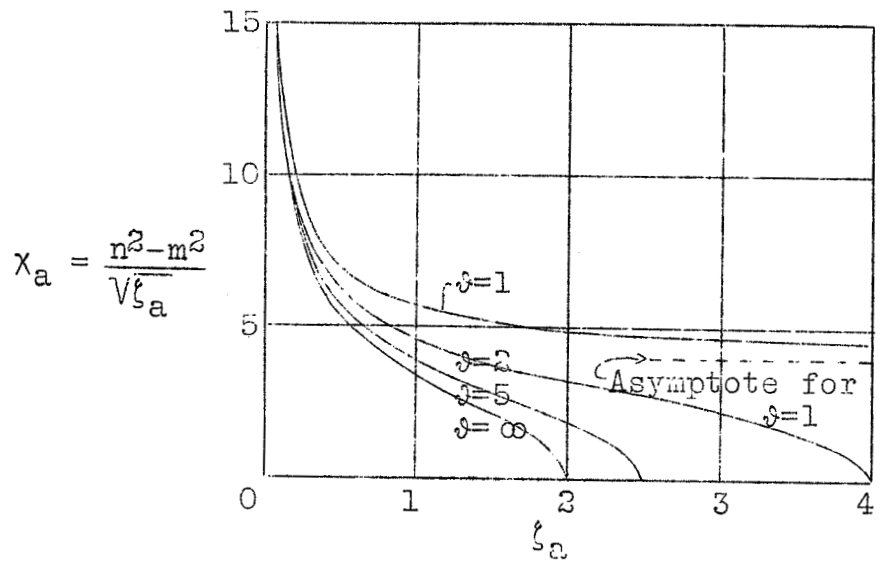

Fig.9a $\chi_a=(n^2-m^2)/\sqrt{\zeta_a}$ plotted against ζ_b and ϑ, $(1 \leqq \vartheta \leqq \infty)$

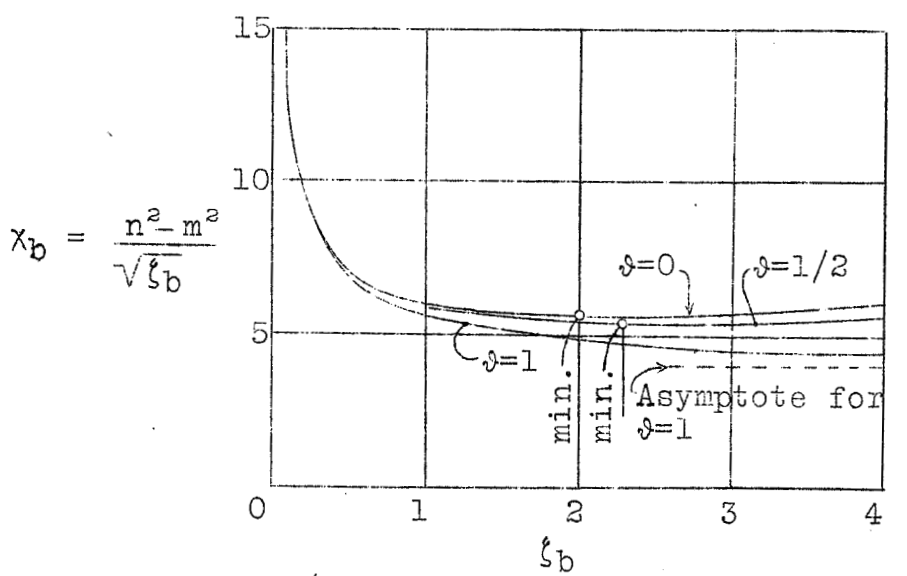

Fig.9b $\chi_b=(n^2-m^2)/\sqrt{\zeta_b}$ plotted against ζ_b and ϑ, $(0 \leqq \vartheta \leqq 1)$.

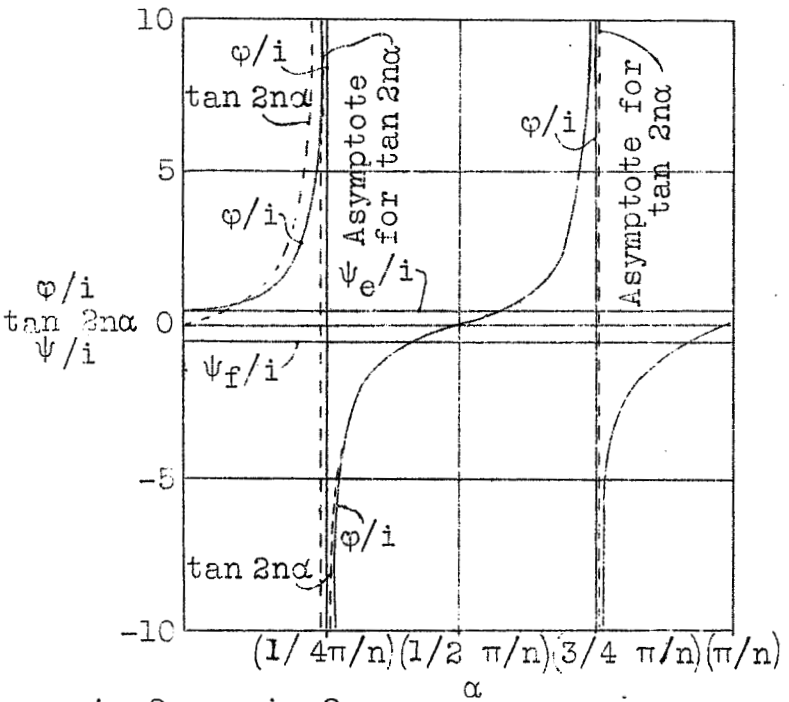

Fig.10 $\varphi/i = \dfrac{\sin 2n\alpha \sin 2\underline{m}\alpha}{\cos 2n\alpha \cos 2\underline{m}\alpha - \cos 4\alpha}$ (=tan 2nα tan 2 $\underline{m}\alpha$ ω) and tan 2 nα as well as ψ_f/i and ψ_e/i plotted against α(see equation 30)

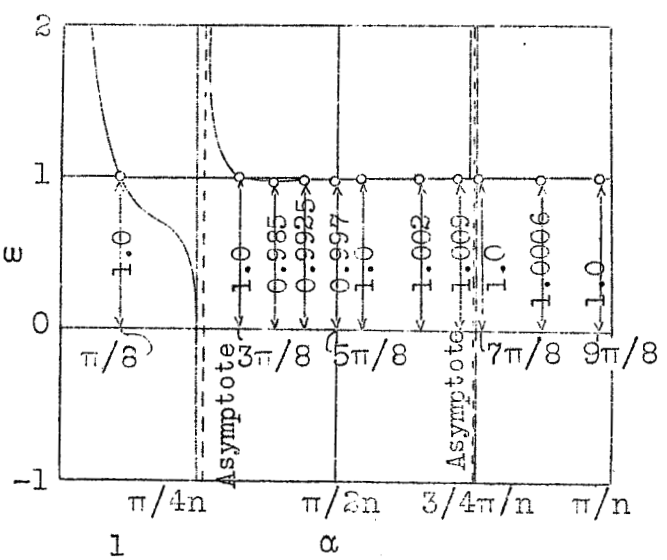

Fig.11 $\omega = \dfrac{1}{1 - \dfrac{\cos 4\alpha}{\cos 2n\alpha \cos 2\underline{m}\alpha}}$ plotted against α for(n.and $\underline{m}$ of Fig.10)

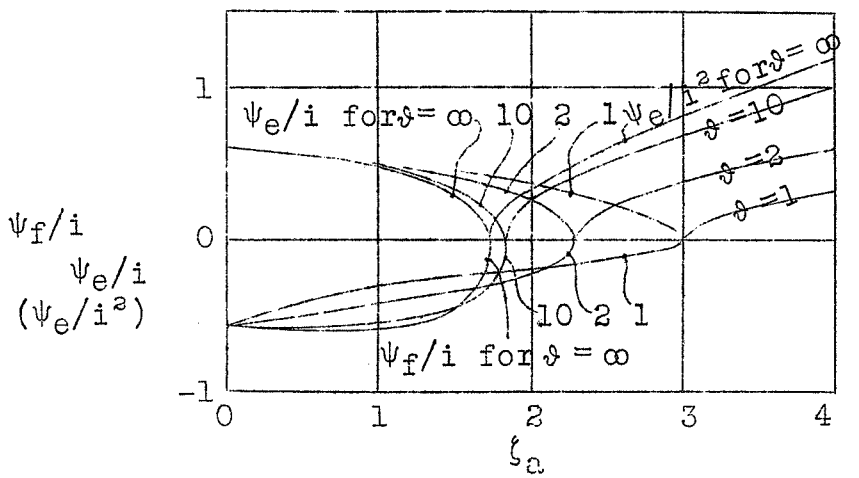

Fig.12a ψ_f/i and $\psi_e/i(\psi_e/i^2)$ plotted against ζ_a and ϑ, $(1 \leqq \vartheta \leqq \infty)$.

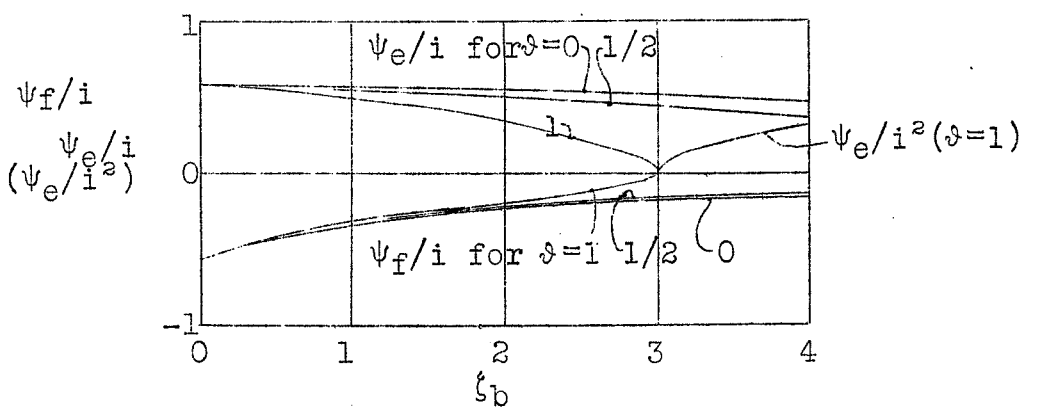

Fig.12b ψ_f/i and $\psi_e/i(\psi_e/i^2)$ plotted against ζ_b and ϑ $(0 \leqq \vartheta \leqq 1)$

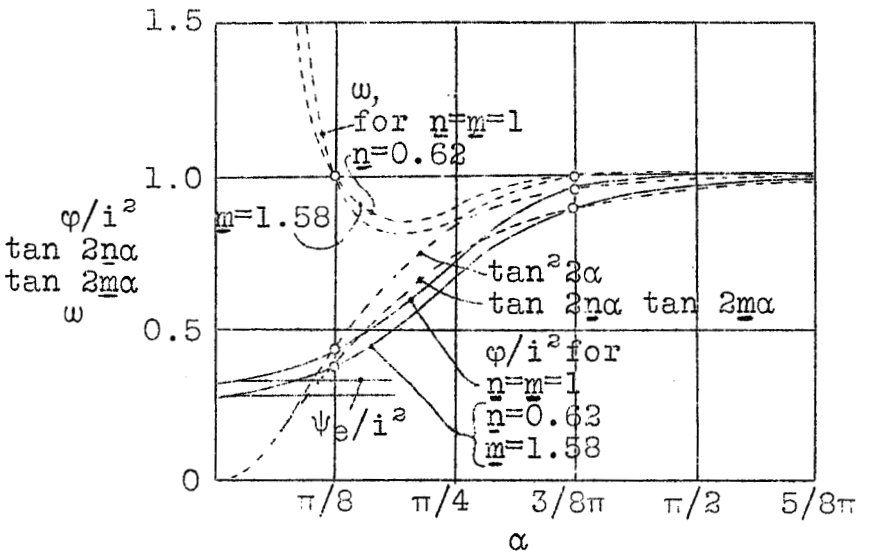

Fig.13 φ/i^2 and tan 2mα tan 2nα and ω plotted against α.

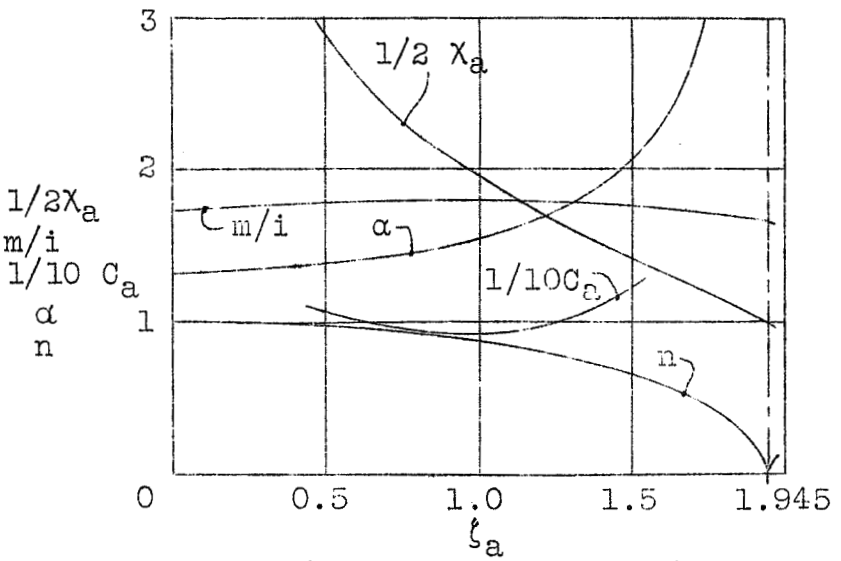

Fig.14 Functions 1/2 χ_a, α, n, m/i and 1/10 C_a plotted against ζ_a for ϑ =5 by rigidly restrained edges.

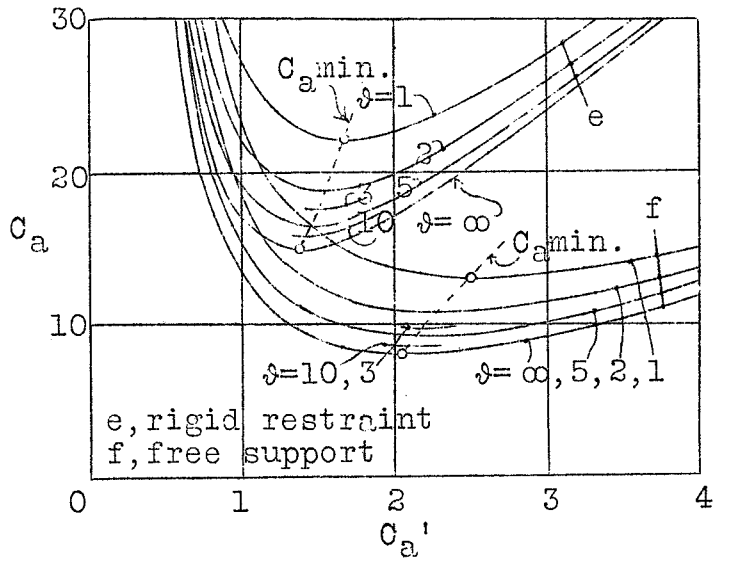

Fig.15a $C_a = t\, a^2/\sqrt[4]{D_1 D_2^3}$ plotted against $C_a' = \frac{l}{a}\frac{1}{\sqrt[4]{\rho}}$

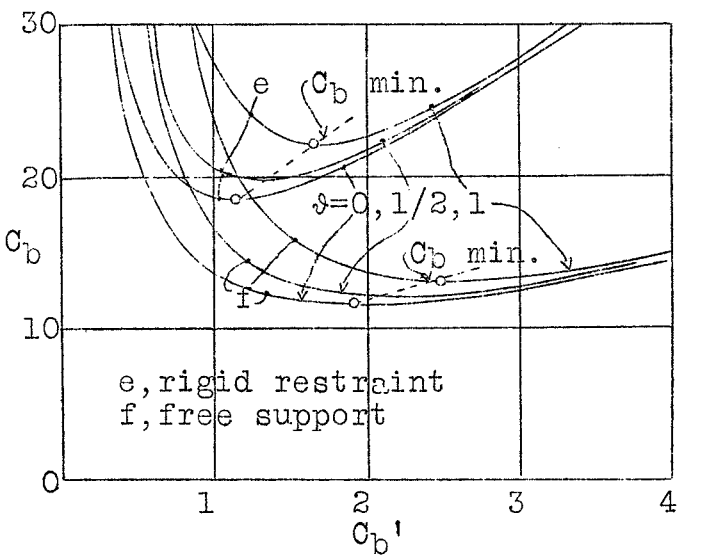

Fig.15b $C_b = t\, a^2/\sqrt{D_2 D_3}$ plotted against $C_b' = \frac{l}{a}\frac{1}{\sqrt{\mu}}$